atmosphere

MDPI

Review

The Vertical Distribution of VOCs and Their Impact on the Environment: A Review

Da Chen [1,2], Yanhong Xu [1,3], Jingcheng Xu [1,3], Meiling Lian [1,2], Wei Zhang [1,2], Wenhao Wu [1,3], Mengying Wu [1,2] and Jingbo Zhao [1,2,*]

[1] Tianjin Engineering Research Center of Civil Aviation Energy Environment and Green Development, Civil Aviation University of China, Tianjin 300300, China
[2] College of Transportation Science and Engineering, Civil Aviation University of China, Tianjin 300300, China
[3] College of Safety Science and Engineering, Civil Aviation University of China, Tianjin 300300, China
* Correspondence: jbzhao@cauc.edu.cn

Abstract: Volatile organic compounds (VOCs) play an important role in atmospheric chemistry. Primary VOCs take part in chemical and photochemical reactions, contributing to ozone (O_3) and secondary organic aerosol (SOA) formation, which may cause air pollution problems. High VOC concentrations might lead to dizziness, nausea, headaches, genotoxicity, reproductive weakness, and other diseases harmful to human health. Several studies have been performed to analyze the components, variations, or sources of VOCs at the ground level. In contrast, studies of the vertical distribution characteristics of VOCs are scarce, and the VOC potential for O_3 formation in the boundary layer is not yet well understood. To better understand the VOC vertical variation regularities and related reasons in temporal and spatial dimensions, thus to deepen the understanding of their effects on O_3 and SOA formation in the vertical direction and to identify the existing gaps in VOC vertical distributions, this study reviewed VOC sampling techniques, VOC vertical distribution characteristics, VOC diffusion models, and effects caused by VOCs. This work can be a valuable reference for decision making regarding environmental and health problems.

Keywords: volatile organic compounds; vertical distribution; sampling technique; O_3 formation potential; temporal and spatial variation

check for updates

Citation: Chen, D.; Xu, Y.; Xu, J.; Lian, M.; Zhang, W.; Wu, W.; Wu, M.; Zhao, J. The Vertical Distribution of VOCs and Their Impact on the Environment: A Review. *Atmosphere* **2022**, *13*, 1940. https://doi.org/10.3390/atmos13121940

Academic Editor: Yoshiteru Iinuma

Received: 20 October 2022
Accepted: 14 November 2022
Published: 22 November 2022

Publisher's Note: MDPI stays neutral with regard to jurisdictional claims in published maps and institutional affiliations.

Copyright: © 2022 by the authors. Licensee MDPI, Basel, Switzerland. This article is an open access article distributed under the terms and conditions of the Creative Commons Attribution (CC BY) license (https://creativecommons.org/licenses/by/4.0/).

1. Introduction

Volatile organic compounds (VOCs) in the atmosphere are complex, and not only they can be emitted directly from the source to the ambient atmosphere, but they can also be generated through photochemical reactions. Some VOCs indirectly affect the natural environment by altering the Earth's atmosphere, resulting in climate change, acid deposition, and other effects. Several VOCs could also lead to chronic lesions of the skin, central nervous system, liver, and kidneys, which seriously threaten human health (Haick et al. [1]). VOCs also are the precursors of ozone (O_3) and secondary organic aerosols (SOAs) [2]. O_3 is the main component of photochemical smog and one of the leading indicators to measure its intensity. Tropospheric O_3 has a non-negligible effect on global warming as an important greenhouse gas. High near-ground O_3 concentrations can irritate the human eye and the respiratory system, cause air quality deterioration, and harm plant growth [3]. SOAs seriously affect lung ventilation function, causing asthma, bronchitis, and other diseases [4]. Many studies have investigated ground-level VOC components, variation, and source apportionment [5]. However, research on VOC distributions in the vertical direction is still scarce [6].

The tropospheric distribution of VOCs depends on many factors, including the emission rates, dispersion, and physicochemical properties of VOCs [7]. VOCs undergo a series of chemical reactions in the atmosphere after emission. The degradation reactions of VOCs result in the generation of intermediate $R\dot{O}_2$ and HO_2 radicals. These $R\dot{O}_2$ and

HO_2 radicals react with NO, converting NO to NO_2 and then photolyzing to form O_3. Thus, the concentrations of O_3 and VOCs show a close relationship at different heights, since VOCs play an essential role in the formation of tropospheric O_3 [8]. Therefore, it is vital to understand the evolution and vertical distribution of VOCs at different altitude levels to solve the urban tropospheric O_3 pollution problem and improve regional air quality. Additionally, the systematic and reliable VOC vertical concentration data also play an essential role in the application of air quality models (e.g., CALPUFF, ADMS, and AERMOD models) for simulating O_3 dispersion in the atmosphere, and system simulation results provide a worthy reference for air quality management [5,9].

This study reviewed VOC sampling techniques, VOC vertical distribution characteristics, VOC diffusion models, and effects caused by VOCs. Among them, the vertical distribution characteristics of VOCs in different seasons and regions were focused on. This review aimed to better understand the VOC vertical variation regularities and related reasons in space- and time-varying dimensions, to deepen the understanding of their effects on O_3 and SOA formation in the vertical direction. Moreover, this work identified the gaps in VOC vertical distributions and could be a valuable reference for decision making related to environmental and health problems.

2. Sources of VOCs in the Vertical Direction

Vehicle exhaust, catering, auto repair, coatings, gasoline vapor, paint, asphalt, industrial and residential coal burning, biomass burning, and the petrochemical industry are the primary, domestic, ground-level VOC sources [10–12]. Transportation, fossil fuel combustion, industrial processes, and solvent utilization contribute significantly [13,14]. With the transformation of industrial structures and related policies, solvent utilization and industrial processes are gradually replacing transportation as the largest source of VOC emission [14,15]. However, vegetation emission was reported to be the dominant VOC source in urban Tianjin, due to the significant number of broad-leaved trees planted here that can generate VOCs [14]. In remote areas, higher levels of AVOCs were related to the long-range transport of pollutants from polluted areas. Mao et al. [16] and Zhang et al. [17] found that the high levels of VOCs measured in the mountainous region were related to the long-distance transmission of surrounding factories' emissions, gasoline-related emissions, solvent use, and fuel combustion.

Vehicle emissions, industrial emissions, fossil fuel combustion, and solvent utilization are the dominant sources of VOCs in the vertical direction. Existing studies mainly investigated VOC sources at different heights using principal components analyses (PCAs) [2,18,19]. Mao et al. [18] and Yang et al. [19] found that the proportion of transportation and industrial emissions increased gradually in the diffusion processes from the surface to the upper atmosphere. This was related to the long lifetime and low reactivity of the components (e.g., isopentane) emitted from gasoline vehicles and via industrial emissions, leading to the slow decrease in concentration with height [2,19]. Wu et al. [2] found that the proportion of coal burning decreased with height. This was mainly related to this source's highly reactive alkenes and aromatics. Additionally, molecular structure and molecular mass are also essential factors that can affect VOC diffusion and transport. For example, Yang et al. [19] found that low-molecular-mass aliphatic hydrocarbons mainly occurred at 500 m, while aromatics with more complex structures and relatively heavy mass usually concentrated at the ground level. Compared with the PCA, positive matrix factorization (PMF) is more suitable for VOC source apportionment due to the non-negative calculation [20]. Many scholars modeled the sources of VOCs in the atmosphere using PMF [21–24]. For example, Yuan et al. [24] measured VOCs at an urban site in Beijing and used PMF to identify emission sources from this VOC data set. The results showed three anthropogenic factors and a biogenic factor [24]. Ling et al. [21] used PMF to analyze the sources of ambient VOCs in Pearl River Delta, southern China, and revealed that vehicular diesel emissions, biomass/biofuel burning, solvent usage, and gasoline evaporation were the dominant

sources there. However, studies using PMF for source-specific analyses of VOC data at different heights are still scarce.

The rapid growth of aviation activities has become another vital source of VOCs vertically [25,26]. Fuel burning in the aircraft taxiing process is the dominant source of VOCs at the level near the airport ground. In this process, the aircraft engine power is limited, resulting in incomplete fuel combustion and HC compound production (mainly alkenes). Hydrocarbon emissions no longer scale to ethene as power increases, and aromatics become the major species emitted. As power increases, combustion processes may change from thermal cracking (which produces mostly alkenes) to forming new molecules (which produces more aromatics). When at cruising altitudes, at around 7000–12,000 m above ground, the engine power drops and remains steady, resulting in lower VOC production [27].

Considering those VOC emission source characteristics in the vertical direction, policymakers could implement effective measures to control VOC pollution from this perspective.

3. VOC Vertical Distribution Sampling Techniques

3.1. VOC Vertical Distribution Samplers

VOC samplers have gone through newer methods, such as gas sampling bags, canister samplers, sorbent-filled tubes, and solid-phase microextraction (SPME) (Table 1). Gas sampling bags have apparent economic advantages over sampling instruments and are easy to operate [28–30]. Tedlar, Kynar, FEP (Teflon), and Fluoride gas sampling bags are often used to collect samples of ambient VOCs (AVOCs) [31–34] (Table 2). However, they have low recovery of non-polar species and easily leak [35,36]. Compared with air sampling bags, the canister-based sampler could increase the sample holding time (up to 30 days) [37,38]. This method is more reliable than others because of the distinct advantages listed in Table 2 [39]. Adsorbent sampling is widely used; these samplers are attached to tethered balloons, towers, and high-rise buildings to collect air samples. Two adsorbents are used to sample VOCs in ambient air: inorganic adsorbents and organic porous polymer adsorbents [40]. Adsorbent sampling is characterized by good adsorption capability and ease of transportation. However, adsorbent tubes are sensitive to moisture content and have low recovery of non-polar species [36]. Solid-phase microextraction (SPME) is typically utilized in aircrafts and consists of fibers (of various kinds) covered with an extracting phase (which can be liquid, solid, or both) to absorb VOCs [41]. SPME is easy to perform, able to be applied in high-risk industrial areas, and friendly towards the environment and human health, and it also costs less in terms of analyses [42,43]. However, sunlight, wind, temperature, humidity, and other prevailing meteorological conditions influence the absorption of VOCs, and the method is unsuitable for sampling high-concentration pollutants [7]. Further details about these four sampling methods are shown in Table 2.

Table 1. Primary information about VOC air samplers.

Sampler	Materials	Operating Principles	Advantages	Disadvantages	Sample Storage Time (Maximum)	References
Air sampling bags	Tedlar, Kynar, FEP, Fluode, etc.	Introduction of air samples into gas sampling bag using tools such as sampling pumps	(1) Light weight (2) Lower cost than canister (3) Easy to transport (4) Reusable	(1) Easily leaks (2) Short sample holding time (3) Long sampling time (4) Not suitable for highly reactive compounds (5) When transported by air or at high altitudes, may break due to reduced atmospheric pressure	24 h	[32,36,44]
Canisters	Summa cans	Automatic gas sample collection through negative pressure in the canister	(1) Easy storage of samples (2) Can be automated (3) Large sample collection volume (4) Long sample storage time (5) Reusable	Proper cleaning of the canister, pump, and flow regulator are required before sampling, otherwise sample contamination occurs	30 days	[36,38,45]
Adsorbent cartridge/tube	The sampling tube is usually made of stainless steel or hard glass	(1) Introduction of air samples into the adsorption tube (2) Rapid heating of the adsorption tube for thermal desorption (3) Analyzed with GC-MS	(1) Better absorption capacity (2) Better effect than canister-type sampler (3) Small size and easy to transport	(1) Affected by moisture content (2) Low recovery of non-polar species	14 days	[36,46]
SPME	Fibers coated with an extracting phase (liquid or solid)	(1) Introduction of air samples into SPME (2) Adsorption of samples using fibers (3) Analyzed with GC-MS	(1) Easy to operate (2) Friendly towards the environment and human health (3) Can be applied in high-risk industrial areas (4) Low cost of analyses	(1) VOC adsorption quantity is influenced by meteorological conditions (sunlight, wind, temperature, humidity, etc.) (2) Not suitable for collecting high-concentration pollutants	15 days	[36,47]

Table 2. Performance comparison of commonly used fluoropolymer film sampling bags.

Performance	Tedlar	Kynar	FEP	Fluode
Thermotolerance (°C)	150~170	150~170	200~260	150~170
Water vapor transmission rate (g m^{-2} 24 h)	12.72	–	1.33	10.9
Oxygen transmission rate (cm^3 cm (m^2 24 h 0.1 pa)$^{-1}$)	114	–	2420	126
Corrosion resistance	Low	Average	High	Average
Adsorption resistance	Average	Average	High	Average
VOC residual degree	Average	Low	High	Low
Mechanical strength	High	Average	Low	High
References	[28,32,36,44,48]	[34,44]	[33,44]	[31,32]

–, not mentioned in the references.

3.2. VOC Vertical Distribution Sampling Techniques

3.2.1. Building-/Tower-Based Measurements

Buildings/towers are commonly built for active sampling with instruments that operate continuously. Flight mass spectrometers (PTR-TOF-MS) are often applied to tower-based measurements [49–51]. For example, Kaser et al. [49] collected air samples on a tower and investigated the interannual variability of terpenoid emissions using PTR-TOF-MS. They found a higher interannual isoprene flux variability than that of other terpenes [51]. Zhang et al. [51] observed the vertical profiles of isoprene and monoterpenes using the proton-transfer-reaction time of PTR-TOF-MS at heights of 3, 15, 32, 64, and 102 m above the ground on a tower in central Beijing and found that the isoprene mixing ratios were more significant in summer due to much stronger local emissions. In contrast, monoterpenes were lower in summer mainly due to their consumption of much higher levels of O_3 [51].

Other instruments, such as sorbent-filled tubes and canisters, can also be applied to sample VOCs at different heights and levels of a building/tower [18,52]. Mao et al. [18] collected VOCs at 8 m, 32 m, 140 m, and 280 m based on a 325 m meteorological tower in urban Beijing using specially designed stainless-steel flasks. Most VOC compound profiles showed a descending trend with the increase in height, except for the thermal inversion layer [18]. Vertical sampling using buildings/towers has the advantage of being easy to operate. Nevertheless, the flexibility of this VOC sampling method is limited because it depends on the height and location of the tower/building [36]. Additional details are shown in Table 3.

3.2.2. Tethered Balloons (Airships)

Tethered balloon measurement mainly refers to the vertical sampling of VOCs by fixing gas sampling bags, canisters, and other instruments to a tethered balloon. This technology has been the most widely used for vertical AVOC sampling [5,53,54]. Wohrnschimmel et al. [55] and Tsai et al. [54] collected VOC samples in the vertical direction using this method and found that propane, butane, and toluene concentrations decreased with the increase in height. Airships provide higher sampling heights than building-/tower-based sampling techniques, with a maximum sampling height of 1600 m being documented in the literature [56]. However, this technique also has some limitations, such as slower speed and short flight distances [36]. Other details about this technique are shown in Table 3.

3.2.3. Aircrafts

Aircraft sampling technology is mainly for continuous measurements. PTR-TOF ONLINE sampling from aircrafts has been developed in several studies [57–59]. For example, Veres et al. [59] measured the anthropogenic sources of VOCs in a football stadium with PTR-TOF-MS and found that human respiration/breath, ozonolysis of skin oils, and cigarette smoke/combustion were the dominant sources [59]. Koss et al. [58] observed VOC emissions and photochemical products over US oil- and gas-producing regions using high–resolution PTR-TOF-MS. They found that aromatics, cyclic alkanes, and alkanes were the typical compounds [58]. Additionally, canisters and SPME can also

be installed on an aircraft to collect air samples [60,61]. Furthermore, aircrafts can also carry sensors to collect meteorological parameters and other air quality data [36]. Using aircrafts for vertical VOC sampling can overcome the limitations of building-, tower-, and balloon-based measurements in terms of sampling heights and locations [62,63]. Currently, the maximum altitude of aircraft sampling is 12 km. Nevertheless, this technique also has some challenges, as shown in Table 3 (e.g., the air samples may be contaminated because of aircraft exhaust emissions; there is a high risk when flying near the ground level; and its economic cost is higher than that of other techniques) [36].

3.2.4. Remote Sensing and Satellites

Remote sensing detects a trace of a specific substance by measuring the absorbance of light at various wavelengths. It has been used to provide reliable data required for air quality modeling and forecasting, emission estimation, monitoring long-occurring air pollutants, etc. [28,64]. Kumar and Viden [28] monitored VOCs at the ground level using a DOAS (differential optical absorption system). Different remote sensing methods are used to examine satellite-taken images to quantify the concentrations of various air pollutants. Many satellite platforms have been set up to perform VOC monitoring, such as ERS-2, ENVISAT, AURA, and METOP-A [65–68]. Jin et al. [69] combined 20 years of $HCHO/NO_2$ data from multiple satellites with ground-based observations to study the chemical changes in ground-level O_3-NO_X VOCs in urban areas of the United States. This technique is advantageous for filling in the gaps left by other monitoring strategies since it can deliver large-scale, high-resolution, real-time data at the regional, national, and even continental levels [65]. However, this technique has more limitations, as listed in Table 3. One of the primary limitations is that satellites only provide columnar data for the entire atmosphere and cannot extract vertical VOC profiles [36].

3.2.5. Unmanned Aerial Vehicles (UAVs)

UAVs equipped with AVOC samplers and sensors have been successfully used for air quality studies, including VOC sampling [70], particulate matter sampling [71,72], ozone observation, etc. [73]. Vo et al. used a UAV equipped with a battery-powered rotor, canisters, and sensors to collect air samples and meteorological data. Samples were collected up to 1000 m, and VOC concentrations decreased with the increase in height, except for the inversion layer. UAVs offer several advantages over aircrafts, such as flexibility in flight schedules and significantly lower costs [74]. Compared with other sampling techniques, UAVs require less space for taking off and landing [75]. The highest sampling height recorded in the literature is 1000 m [71]. Although UAVs have some disadvantages, as summarized in Table 3, they still have the highest potential to be more widely used in future AVOC research due to their advantages over other methods [36]. For instance, according to the USEPA TO-15 Method, canisters can be readily retrofitted with UAVs that can measure more than 100 VOC species at low concentrations (ppb). UAVs can be integrated with reliable, high-quality sensors to provide high-resolution air pollutant data and meteorological parameters. These 3D monitoring data can be sent to a cloud server for post-processing, and Global Information System (GIS) mapping techniques can be used to generate high-resolution temporal–spatial air quality maps for supporting the decision-making process [73,76].

3.3. VOC Analytical Techniques

Gas chromatography–flame ionization detection (GC-FID) and gas chromatography–mass spectrometry (GC-MS) are two crucial gas chromatography (GC) techniques used for the analysis of VOCs. Especially, GC-MS is a powerful analytical technique in the study of VOCs owing to the vital identification function of mass spectrometry (MS). To date, many researchers have investigated the components and concentrations of VOCs in the atmosphere with promising results [77,78]. However, this method has many limitations. For example, this method is applied mostly offline, with a significant time lag. Moreover,

the pretreatment of complex samples is time consuming, laborious, and economically costly [79,80].

In recent years, proton-transfer-reaction mass spectrometry (PTR-MS) has emerged as a valuable tool for studying VOCs in the atmosphere [80]. As mentioned in 2.2, PTR-TOF-MS is commonly used with tower and aircraft sampling techniques to study VOC concentration characteristics in the atmosphere at different altitudes [51,57–59]. This online method could overcome the disadvantages of offline methods and has the advantages of high resolution, high sensitivity, and short monitoring time [80,81]. However, PTR-MS can only distinguish ions by their nuclear-to-cytoplasmic ratio, so it is challenging to distinguish isomers [82].

Table 3. VOC vertical distribution sampling techniques.

Technology	Commonly Equipped Instruments	Maximum Sampling Height	Advantages	Disadvantages	References
Building-/tower-based measurements	(1) PTR-TOF-MS (2) Adsorbent cartridge/tube (3) Canister	About 280 m	(1) High-resolution data (2) Shorter monitoring time (3) Being steady and long-term observation	(1) Fixed position (2) Low sampling height	[18,51,52,83–85]
Tethered balloons (airships)	(1) Air sample bag (2) Canister	About 1600 m	(1) Low cost compared with aircrafts (2) Can hover for a long time with better stability performance and long-term observation	(1) Requires a large landing space (2) It is difficult to control height and position (ascent height is related to fuel content) (3) Slow moving speed (about 80–100 m/h)	[19,55,56,86]
Aircrafts	(1) PTR-TOF-MS (2) Canister (3) SPME (4) A novel whole-air sample profiler (WASP), etc.	About 12 km	(1) Higher sampling height (2) Multifunctional—can carry SPME, WASP, and other instruments (3) High-resolution data (4) Shorter monitoring time	(1) Aircraft exhaust emissions may cause cross-contamination of samples (2) Higher risk when flying below 500 m (3) High cost due to human and material investment, such as pilot and aircraft maintenance	[30,60–63,87,88]
Remote sensing and satellites	/	/	(1) Regional, national, and even continental scale monitoring is possible (2) Large-scale, high-resolution, real-time data are available	(1) Only a small number of compounds, such as glyoxal, methanol, peroxyacetyl nitrate, and formaldehyde, can be detected (2) Strongly affected by the atmospheric conditions (3) Cost and risk of launching satellites are high (4) Only provide columnar data of the whole atmosphere, unable to extract vertical VOC profiles	[28,36,65]
UAVs	(1) Canister (2) SPME (3) WASP, etc.	About 1000 m	(1) Flexible sampling altitude and low risk of near-ground flight (2) In addition to SPME, WASP, and other instruments, can also carry meteorological sensors, etc. (3) Flexible sampling time (4) Low cost compared with aircrafts (5) Small takeoff and landing space	(1) Limited battery power and short operating time (2) The external coating of the UAVs may cause cross-contamination of the sample (3) Few types of sensors can be chosen (4) Inadequate laws and regulations regarding the operation of UAVs	[73,76,89–91]

/, not recorded in the references.

4. Vertical Distribution Characteristics of VOCs

4.1. Temporal Variations in the Vertical Distribution of VOCs

4.1.1. Diurnal Variations in the Vertical Distribution of VOCs

The diurnal variation characteristics of the vertical distribution of VOCs are different on clear days and haze days. In general, the concentrations of total volatile organic compounds (TVOCs) and most components tend to decrease with the increase in height (except for the inversion layer) on both clear and haze days. However, Mao et al. [18] observed a particular case in which aromatic (mainly toluene) concentrations exhibited an increasing trend with the increase in height from 8 to 140 m at 10:00 p.m. and then a decreasing trend from 140 to 280 m (Figure 1c). This phenomenon may be related to the high concentration of OH radicals at 140–280 m, which promoted the removal process of aromatics.

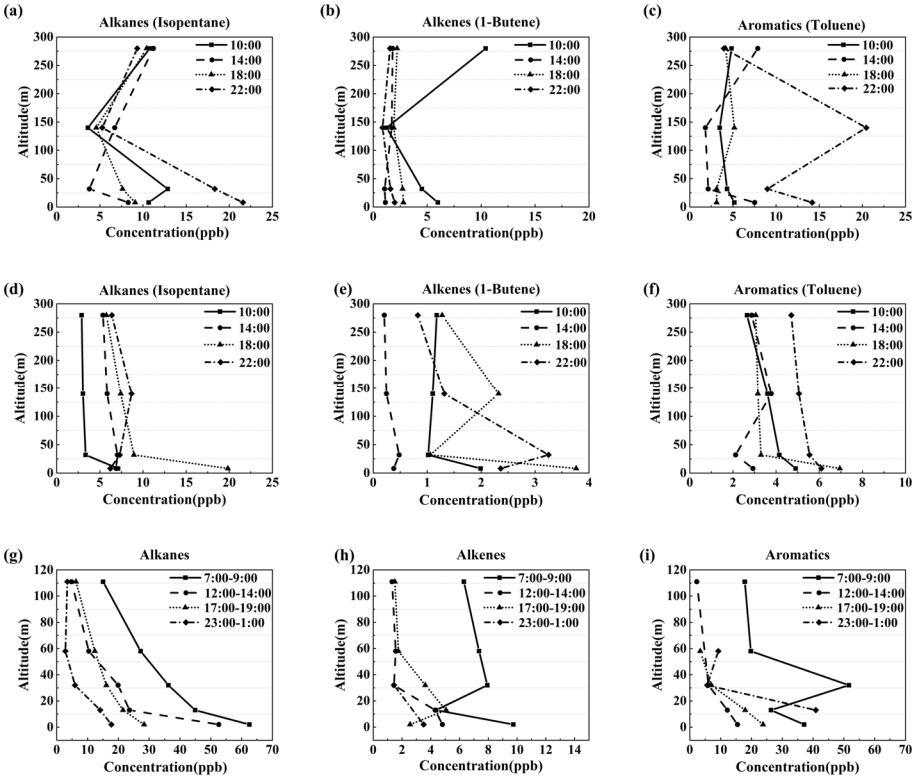


Figure 1. Average profiles of vertical distributions of VOCs in (**a**–**c**) Beijing haze days, (**d**–**f**) Beijing clear days, and (**g**–**i**) Kaohsiung clear days [18,83].

The morning rush hours from 7:00 to 9:00 a.m. are typically when VOC concentrations are at their highest. These are followed by the evening rush hours from 5:00 to 7:00 p.m., the hours between 12:00 a.m. and 2:00 p.m., and the hours between 11:00 p.m. and 1:00 a.m. (Figure 1), indicating that most VOC compounds in urban air originate from traffic and transportation emissions. The low atmospheric mixing height in the early morning may lead to insufficient vertical mixing, making VOC vertical dilution less possible than at other times of the day [18,92].

The vertical variation in TVOC concentrations is more significant on haze days, while the variation in VOC concentration is more significant at different times on clear days (Figure 1). It is due to differences in the altitude of the thermal inversion layer on clear days, and the reaction activities of different components vary with the temperature and solar radiation. These factors eventually lead to more detailed vertical profiles at various times on clear days. For example, Mao et al. [18] found that the alkenes (mainly 1-butene) vertical profiles at 10:00 a.m. and 6:00 p.m. were consistent and showed a decreasing tendency with the increase in height from 8 to 32 m and an opposite tendency from 140 m

to 280 m due to the occurrence of the inversion layer. At 2:00 p.m. and 10:00 p.m., VOC concentrations decreased with the increase in altitude in general (Figure 1e). For alkane (mainly isopentane) and aromatic (mainly toluene) concentrations, they decreased with the increase in height, except at 10:00 p.m., and the concentrations of alkanes reached their highest at 10:00 p.m. when the altitude was up to 140 m (Figure 1d). Additionally, alkane chemical properties are more stable than those of alkenes. They do not efficiently react with other compounds throughout the atmospheric transport process, resulting in higher alkane concentrations at 140 m [18]. Lin et al. [83] discovered that TVOCs and most components showed a decreasing trend with the increase in height in almost all periods during the day (Figure 1g–i). However, between 7:00 to 9:00 a.m., alkenes and aromatics concentrations increased with the increase in height from 13 to 32 m (Figure 1h,i). Temperature reversion can explain this phenomenon, which restricted the vertical dispersion of VOCs between 13 and 32 m. Furthermore, a significant number of aromatics emitted from industrial sources near the sample site during this time was another crucial cause. During the hours from 5:00 to 7:00 p.m., alkenes showed an increasing trend with the increase in height from the surface to 13 m (Figure 1 h). Although the causes for this discovery were unclear, it seemed likely that these particular VOCs were caused by local industrial sources rather than by emissions from vehicles and traffic [83].

4.1.2. Seasonal Vertical Distribution Characteristics of VOCs

TVOC concentrations are generally higher in winter than in summer [93,94]. The concentrations of TVOCs in spring and autumn are between those in winter and summer. It is because the concentration of the hydroxyl (OH) radical is relatively high in summer, which increases the rate of NMHC removal from the atmosphere. Since the reactivity of VOCs generally decreases with the decrease in the temperature, VOCs react with more difficulty under winter conditions [42,95,96].

TVOC concentrations generally decrease with the increase in height in the four seasons due to anthropogenic emission sources being primarily accumulated at the ground level [97]. Nevertheless, the vertical distribution of specific VOC components is more complex between seasons (Figure 2). For example, Zhang et al. [98] observed the vertical distributions of VOCs within 1000 m during late spring using a tethered balloon and found that alkanes accounted for 44.83% of TVOCs at the ground level but up to 67.90% at 50–350 m. In comparison, aromatics are active and easily converted to other compounds. Thus, the contribution of TVOCs tends to decrease at higher altitudes (Figure 2a). Cabañas et al. [99] found that the proportion of aromatics decreased at higher altitudes on clear days, while it increased at higher altitudes on haze days (Figure 2b,c). One possible reason for the increased proportion of aromatics at high altitudes on haze days is as follows: The only necessary removal process for aromatics is their reaction with OH radicals during the day [97], and this process is weakened, as the OH radical level is lower at higher altitudes due to the elevated NO levels close to the ground, which leads to the accelerated conversion of HO_2 into OH [18,98]. This tendency for aromatics contrasts with alkanes, which react with OH radicals and another significant atmospheric oxidant, the Cl atom [99]. The concentration of VOC components changes more significantly in winter than in summer (Figure 2d,e). That is, the atmospheric stratification is more stable in winter, which is not conducive to the dilution and diffusion of pollutants, allowing pollutants to accumulate [42,95,96]. The intense atmospheric convection and the higher planetary boundary layer (PBL) height in summer lead to a more uniform distribution of VOC concentrations at different altitudes [2]. The concentration of halohydrocarbon in winter decreases significantly with the increase in altitude, while alkanes show an opposite trend (Figure 2d). It is mainly related to the higher proportions of vehicular gasoline emissions, emissions and industrial sources, and coal burning in winter [2].

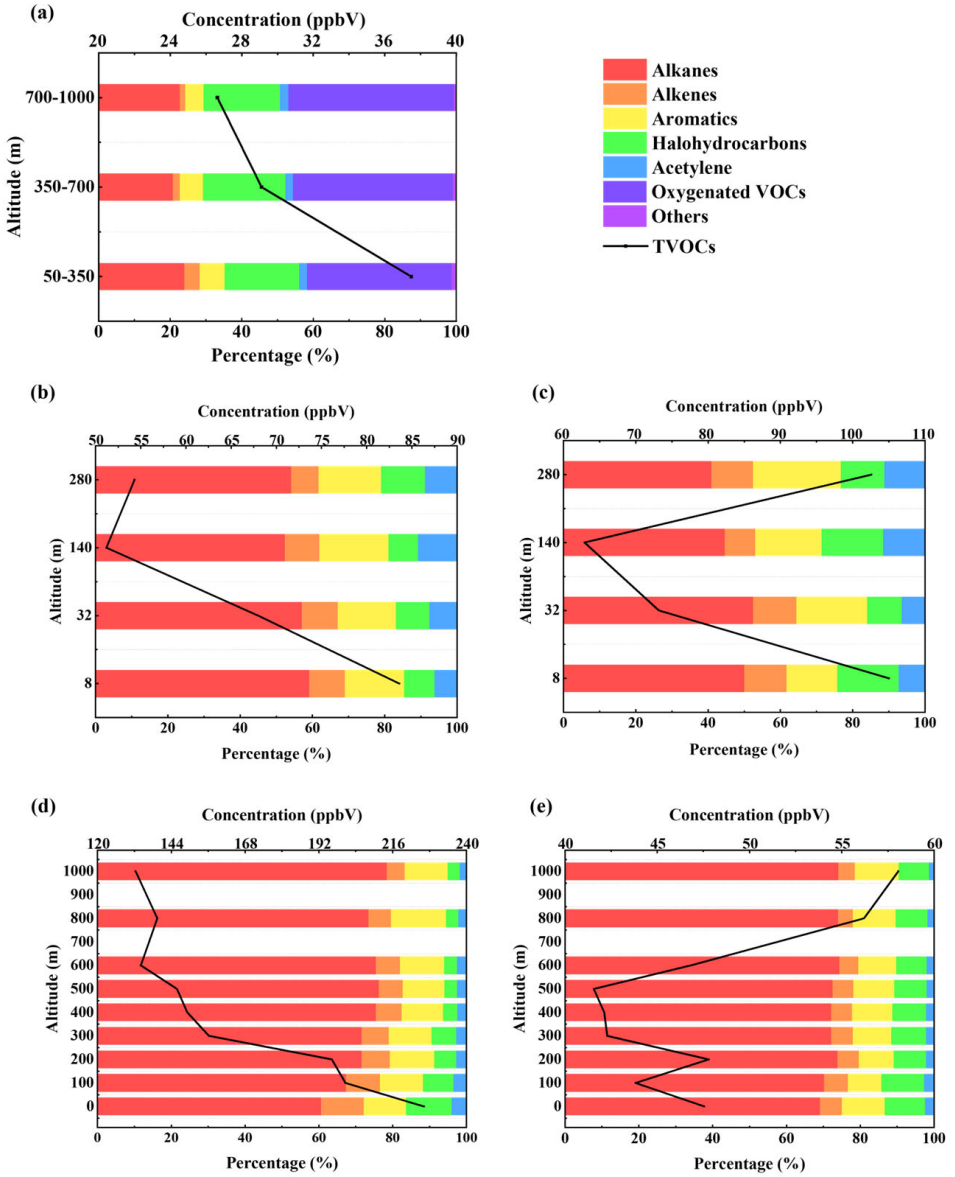


Figure 2. Vertical profiles and proportions of the average concentrations of VOCs in (**a**) late spring in Shanghai [98], (**b**) autumn in Beijing on clear days [18], (**c**) autumn in Beijing on haze days [18], (**d**) winter in North China Plain [2], (**e**) summer in North China Plain [2].

4.2. Regional Vertical Distribution Characteristics of VOCs

4.2.1. Urban and Suburban

The predominant components of suburban VOCs are isoprene, aldehydes, and ketone, mainly emitted from terrestrial vegetation [13]. Most distribution profiles of suburban biogenic VOCs (BVOCs) show a descending trend with the increase in height. However, the profiles of specific components are different. Ieda et al. [52] investigated the vertical distributions of VOCs in a larch forest and found that the concentration of isoprene decreased with the increase in height from the surface to 22 m; then, it increased again above the canopy level (about 22 m), due to the forest floor and the upper canopy being mainly sinks of isoprene [52]. Lower AVOC concentrations can also be observed in suburban areas due to long-distance transportation from urban areas. Liu et al. [100] investigated the vertical distribution of VOCs in the suburbs of Shanghai using a UAV equipped with summa canisters and found that alkanes, aromatics, and alkenes dominated the TVOCs in this area. Both of these three dominant species mainly originated from the nearby factory. The contribution of alkanes and alkenes to TVOCs shows a tendency to decrease with the

increase in altitude. At the same time, aromatics tend to increase, mainly related to the chemical reaction of aromatics with OH mentioned above [100]. Das et al. [101] also found similar characteristics in suburban North Carolina (Figure 3).

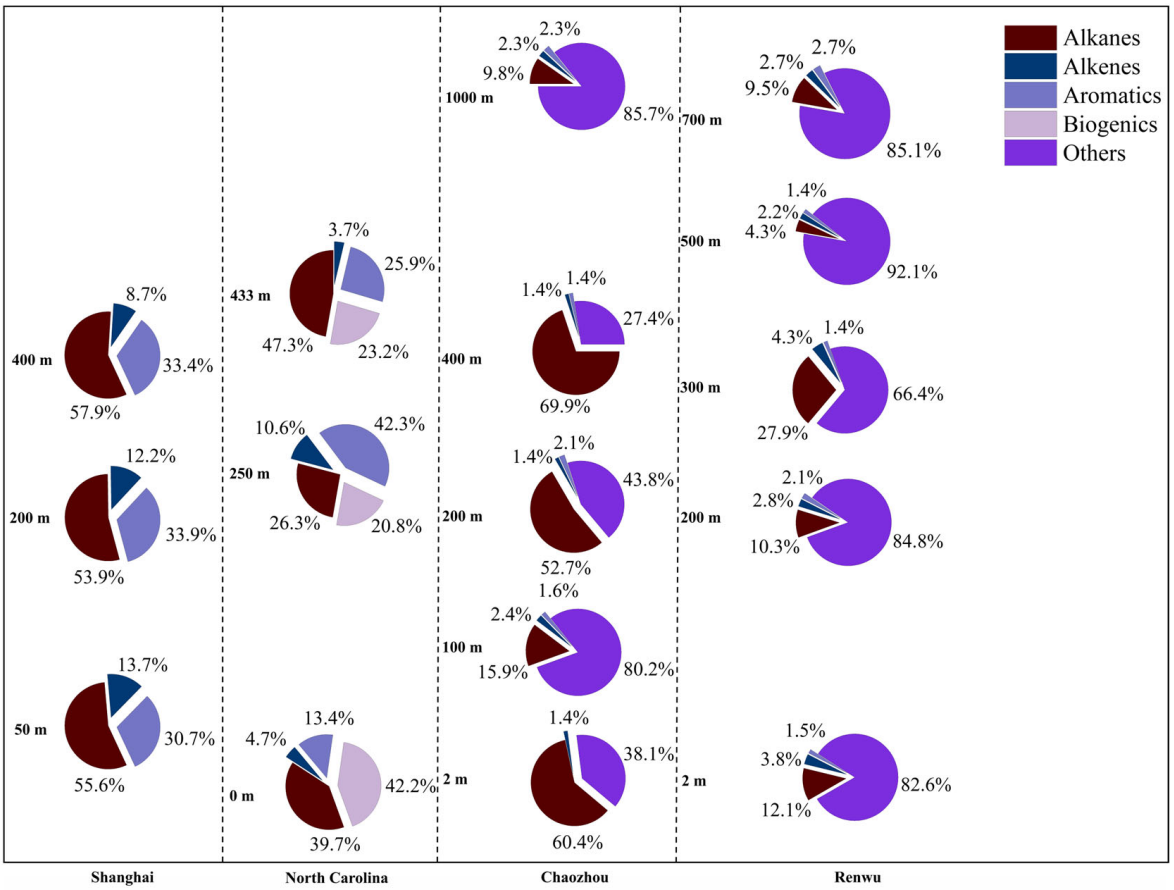


Figure 3. The contribution of each category of VOCs to TVOC concentrations in rural areas (Shanghai [100] and North Carolina [101]) and urban areas (Chaozhou and Renwu [89]).

AVOC concentrations in urban areas are significantly higher than those in suburban areas due to the more concentrated anthropogenic emission sources (e.g., traffic emissions, industrial emissions, fossil fuel combustion, etc.). Vo et al. [89] collected vertical air samples up to 1000 m in Renwu and Chaozhou areas. They found that TVOC concentrations reached the highest (75 ppb) at 400 m in Chaozhou and 300 m (327 ppb) in Renwu [89]. The contribution of each component to TVOC concentrations can be seen in Figure 3. They noted that other than local vehicular exhaust, long-distance transport upwind sources might also have influenced the measured TVOC concentrations. Lin et al. [83] performed similar research in Kaohsiung and found that the VOC concentrations decreased with the increase in height from the surface to 110 m. This observation was mainly due to the short distance between the surface and traffic emissions, which led the pollutants to accumulate near the ground level [83].

4.2.2. Coastal and Inland

The VOC concentrations across the relatively slight economic growth gap between inland and coastal regions also reveal significant differences. Alkanes and aromatics contribute more to TVOCs in inland regions, while alkenes and halocarbons account for a smaller proportion. Using tethered balloons, Geng et al. [6] measured the vertical distribution of VOCs in the Beijing–Tianjin–Hebei region. They found alkanes, alkenes, and aromatics, and oxygenated VOCs (OVOCs) were the dominant components. Additionally, the TVOC concentration at 50–100 m (46.9 ppb) was 4.9 times higher than at 900–1000 m

(8.0 ppb). Moreover, the concentration changed rapidly from the altitudes of 50–100 to 401–500 m, dropping to less than 30% of the original concentration. Among them, aromatic concentrations dropped the fastest (below 20%) from 50 to 500 m, followed by alkanes and OVOCs (below 30%), alkenes (below 40%), and hydrocarbons (below 50%). Additionally, the concentration decreasing rate for each component between 500–1000 m and 50–500 m was different, with aromatics reducing to less than 50%; alkenes, OVOCs, and hydrocarbons all reducing to less than 60%; and alkanes reducing to less than 70% [6].

VOC compositions and concentrations in coastal and inland areas are similar. Nevertheless, the changes in coastal areas are not noticeable in terms of vertical distribution, mainly because of the land–sea breeze. The sea breeze is a thermally induced local circulation that forms due to the differential heating of land and water [102]. Numerous studies have shown that air pollution in coastal areas can readily result from land–sea breeze circulation [103]. It is mainly due to sea breeze, which transports the polluted air masses from the ocean to the inland area [104]. From a dynamic perspective, due to shearing between the seaward synoptic wind and the landward gravity current, local contaminants may move back to the sea above the gravity current at a relatively slow rate. Such dynamic conditions may enhance an accumulation of pollutants above coastal industrial areas [105]. This results in high pollutant concentration levels in coastal areas and in the high-altitude atmosphere. Flocas et al. [60] observed elevated VOC concentrations (150–350 ppb) from 300 to 400 m above the ground level. When the altitude reached 1400–1600 m, VOC concentrations remained relatively high (100–200 ppb). The proportion of alkanes, aromatics, and alkenes declined with the increase in height in the lower altitude range. When the altitude exceeded 1108 m, the aromatic concentrations tended to increase. When the altitude exceeded 1271 m, alkanes also tended to increase. However, the concentration of each component did not change rapidly in the vertical direction due to the sea breeze circulation in this area [60].

5. VOC Vertical Distribution Models

Systematic and reliable VOC monitoring data play a primary role in applying air quality models for simulating O_3 dispersion in the atmosphere. System simulation results provide a valuable reference for air quality management [36]. Models such as AERMOD, ADMS, Models-3 CMAQ, CALPUFF, and WER-Chem are used to simulate VOC dispersion (Table 4).

AERMOD (AMS/US EPA) is a near-field, steady-state, Gaussian plume model based on planetary boundary layer turbulence structure and scaling concepts [9]. AERMOD consists of a meteorological preprocessor (AERMET) and a terrain preprocessor (AERMAP). The AERMOD algorithms have been streamlined, e.g., the treatment of terrain, so the model runs relatively quickly compared with ADMS. Hanna et al. [106] compared the result of AERMOD with five sets of fields and found that the model performed well overall. However, it also had the limitation of underpredicting the mean and maximum concentrations. To ensure that the results are reasonable, Holmes and Morawska [9] noted that modeling with the AERMOD model requires basic assumptions of the Gaussian plume model, such as the steady-state emission source, moderate wind speed, and moderate wind direction changes that are continuous.

ADMS is an advanced steady-state, Gaussian-like dispersion model. The model uses conventional meteorological elements to define the structure of the boundary layer and can better describe the atmospheric dispersion process. ADMS is especially appropriate for simulating atmospheric dispersion from elevated point sources. Although ADMS is similar to AERMOD in many aspects, there are still significant discrepancies in the criteria for input meteorology since AERMOD allows vertical wind and temperature profiles to be obtained. At the same time, ADMS requires one level of near-ground data. Additionally, the ADMS performance is slightly better than the AERMOD performance [107].

The Models-3 CMAQ modeling system has evolved from several models operated at EPA, such as RADM, SAQM, UAM, and ROM [108]. This modeling system comprises three modeling components (Models-3): a meteorological modeling system for describing

atmospheric states and motions, emission models for anthropogenic and natural emissions injected into the atmosphere, and a chemistry-transport modeling system for simulating chemical transformation and fate [109]. Compared with other systems, it has the distinct advantages of simulating on a larger spatial scale and simulating more types of pollutants (up to more than 80 species, as recorded in the literature). However, due to the complexity of the model's algorithm, the calculation speed is relatively slow [109,110].

CALPUFF is a multi-layer, non-steady-state, puff dispersion model designed to model the dispersion of gases and particles [9]. The model can predict pollutants from a few kilometers to several hundred kilometers. Furthermore, CALPUFF can perform better than AERMOD in dealing with the wind direction. Kwak et al. [111] used this modeling system to calculate VOC concentrations. In their study, topography data were mainly acquired from a GIS application. In contrast, meteorological data were derived from 70 surface stations located throughout South Korea and 1 upper-air station. The modeling results not only clearly described the spatial concentration ranges of benzene (0.001–8.27 μg m^{-3}), ethylbenzene (0.001–3.19 μg m^{-3}), styrene (0.001–7.83 μg m^{-3}), toluene (0.01–83.8 μg m^{-3}), and xylene (0.005–66.8 μg m^{-3}) but also found that the VOC concentrations were higher in urban regions with high population densities than in rural regions in almost all cases. However, the model is inadequate for simulating pollutant dispersion when the timescale is less than one hour or when the diffusion is substantially influenced by turbulence, as in an urban setting. Furthermore, it has a low temporal agreement and underpredicts pollutant concentrations [9].

WRF-Chem is a regional air quality model developed by NOAA/ESRL (National Oceanic and Atmospheric Administration/Earth System Research Laboratory). The model has the same grid structure on the air quality scale and meteorological scale, with no temporal interpolation, and is suitable for simulating meteorological–chemical feedbacks (climate change) from local to global scales and air quality conditions from the cloud scale to various weather scales [112,113]. Unlike the Models3-CMAQ model, the meteorological and chemical processes are carried out separately in WRF-Chem. WRF can simulate high-resolution numerical simulations in the 1–10 km range. Chem can simulate pollutant transport and dispersion, wet and dry deposition, gas-phase chemical reactions, source emissions, photo-decomposition, aerosol dynamics, and aerosol chemistry [107]. Chutia et al. [114] compared the WRF-Chem-simulated values of VOC dispersion with the ground-based observations over India. They ultimately found that the WRF-Chem simulations for acetone, acetaldehyde, and toluene were reasonable. However, the model overestimated propane over high-altitude sites and urban stations. This bias was mainly due to the inadequate description of the regional-scale topographic resolution (including forests, hills, and mountains) and the uncertainty of anthropogenic emissions [114]. Long calculation time and poor flexibility are the other limitations of WRF-Chem [112].

In summary, different VOC vertical dispersion models exhibit various performances in practical scenarios. Critical challenges to applying these models are the uncertainties of the model-predicted concentrations due to the lack of systematic and reliable VOC monitoring data. Comparing these models from the view of the complexity of the environment in the study area, the dimensions of the model, the character of the particle, the accuracy calculations, and the time scales, the Models-3 CMAQ model performs relatively better, and it can simulate primary pollutants on a larger spatial scale and under more complex weather conditions. Additionally, it combines more abundant functions with tropospheric ozone and acid deposition to provide technical support for air quality forecasting, assessment, and decision making. Therefore, this model has promising application.

Table 4. VOC vertical distribution models.

Model	Type	Applicable Scenarios	Simulable Pollutants	Grid Size	Advantages	Disadvantages	References
AERMOD	Bi Gaussian steady-state GP	(1) Dispersion simulation of pollutants on local, urban, and regional scales is possible (2) Point sources, surface sources, and volumetric sources can be modeled (3) Simulation of ground-level sources and elevated point sources is possible (4) Simulation can be performed for both flat terrain and complex terrain	(1) SO_2, NO_2, VOCs, and other primary pollutants (2) Fine particulate matter	<50 km	(1) Advanced algorithms to describe turbulent mixing processes in the troposphere and steady layer in the planetary boundary layer (2) Plume rise and buoyancy can be calculated to describe the vertical profiles of wind, turbulence, and temperature (3) The algorithm is more simplified and runs faster than ADMS	(1) Underestimation of the average and maximum of pollutant concentrations	[9,106,115]
ADMS	3D quasi-GP	Similar to the AERMOD model and especially suitable for the simulation of pollutant dispersion from elevated point sources	(1) SO_2, NO_2, VOCs, and other primary pollutants (2) Secondary pollutants such as sulfate, nitrate, and O_3 (3) Fine particulate matter	3000 grid cells up to 50 km	(1) Requirements for meteorological data are lower, and simulation process is simpler (2) The latest knowledge of physical parameters of atmospheric structure is used (3) The prediction performance of pollutants is slightly better than AERMOD	(1) Underestimation of pollutant concentrations	[106,116]
Models-3 CMAQ	Eulerian grid model	(1) Simulations can be performed on local, urban, regional, and continental scales (2) Various chemical and physical processes of atmospheric pollutants can be simulated (3) Can be used for forecasting, assessment, and decision-making studies of air quality for multiple pollutants	(1) SO_2, NO_2, VOCs, and other primary pollutants (2) Secondary pollutants such as sulfate, nitrate, and O_3 (3) Fine particulate matter	Each domain grid cell is 36 km by 36 km	(1) Larger spatial scale (2) More types of pollutants can be simulated (3) Richer functionality and applications (4) Better performance in the current study	(1) Underestimation of organic carbon concentration (2) Slower calculation speed	[108,109]
CALPUFF	Multilayer, non-steady-state GPuff	(1) Can simulate the dispersion, transport, and deposition of pollutants on a moderate scale from tens of meters to hundreds of kilometers (2) Multiple sources of different types can be modeled (including point, line, and volume sources) (3) Particularly suitable for the simulation of pollutants in special wind-field environments	(1) SO_2, NO_2, VOCs, and other primary pollutants (2) Secondary pollutants such as sulfate, nitrate, and O_3 (3) Fine particulate matter	<200 km	(1) Can simulate the diffusion process of pollutants under some non-stationary conditions (2) Analysis of the initial guess wind field using terrain dynamics and slope flow parameter methods is suitable for simulation under rough and complex terrain conditions	(1) Underestimation of pollutant concentrations (2) Not applicable to the simulation of pollutant dispersion in a turbulent environment (3) Not applicable to the simulation of pollutant dispersion on time scale of less than 1 h	[9,117]

Table 4. *Cont.*

Model	Type	Applicable Scenarios	Simulable Pollutants	Grid Size	Advantages	Disadvantages	References
WRF-Chem	Weather Research and Forecasting model coupled with Chemistry model	(1) Chemistry–meteorology feedbacks from local to global scales can be simulated (2) Air quality can be simulated from cloud scale to various weather scales	(1) NO_X, CO, VOCs, and other primary pollutants (2) Secondary pollutants (O_3, etc.) (3) Fine particulate matter	/	(1) Has a sophisticated photolysis scheme and a state-of-the-art aerosol module to simulate a more realistic atmospheric environment (2) Is more capable of simulating O_3	(1) Underestimation/overestimation of pollutant concentrations (2) Poor modeling flexibility (3) Slower calculation speed	[107]

/, not recorded in the references.

6. The Effect Caused by VOCs

6.1. Atmospheric Chemistry of VOCs in the Troposphere

VOCs oxidize themselves by reacting with OH radicals under light conditions and allow the vital intermediates $R\dot{O}_2$ and HO_2 to form in the atmosphere. $R\dot{O}_2$ and HO_2, as crucial intermediates in the reaction chain, play an essential role in producing other compounds (Figure 4). $R\dot{O}_2$ radicals and HO_2 radicals in the atmosphere react rapidly with NO, converting NO to NO_2, as shown in reactions (1) and (2). $R\dot{O}_2$ radicals react more rapidly, with a reaction rate of about $(7-10) \times 10^{-12}$ $cm^3molecule^{-1}s^{-1}$ [118,119].

$$R\dot{O}_2 + NO \rightarrow R\dot{O}_2 + NO_2 \quad (1)$$

$$HO_2 + NO \rightarrow OH + NO_2 \quad (2)$$

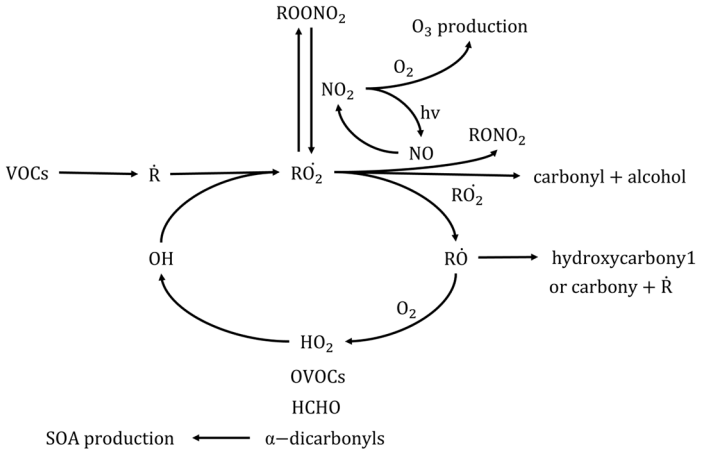


Figure 4. Main VOC chemical reaction processes in the troposphere.

$R\dot{O}_2$ also reacts with HO_2 to produce organic hydroperoxides (ROOH) and oxygen at a reaction rate of about 10^{-11} $cm^3molecule^{-1}s^{-1}$. The reaction has a significant negative temperature effect [119,120].

O_3 is formed photochemically from the photolysis of NO_2; then, NO_2 photolyzes to form NO and $O(^3P)$ atoms, as shown in reaction (3).

$$NO_2 + hv \rightarrow NO + O(^3P) \quad (3)$$

On the one hand, $O(^3P)$ atoms further react with O_2 in air to form O_3, as shown in reaction (4).

$$O(^3P) + O_2 + M \rightarrow O_3 + M \quad (4)$$

On the other hand, O_3 generates NO_2 and O_2 again with the participation of NO, as shown in reaction (5).

$$NO + O_3 \rightarrow NO_2 + O_2 \quad (5)$$

This mechanism leads to a photochemical balance among NO, NO_2, and O_3, with no net formation or loss of O_3, as seen in Figure 5a. However, when reactions (1) and (2) occur in the presence of VOCs in the atmosphere, it increases NO_2 concentrations and breaks the photochemical balance of O_3, as seen in Figure 5a, making NO_2 convert to the direction of O_3 production; thus, net O_3 formation occurs [121]. The processes are shown in Figure 5b.

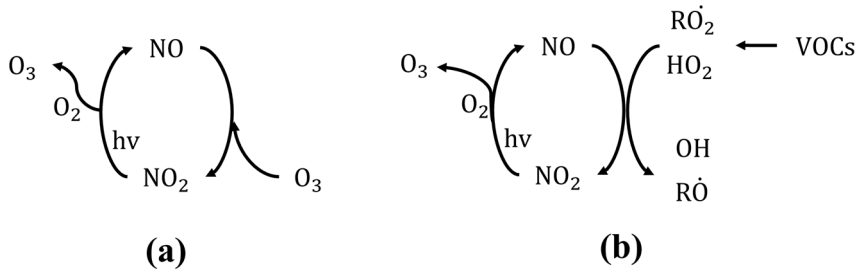


Figure 5. Schematics of the reactions involved in NO-to-NO_2 conversion and O_3 formation in (**a**) NO-NO_2-O_3 systems in the absence of VOCs and in (**b**) NO-NO_2-O_3 systems in the presence of VOCs.

Furthermore, NO and NO_2 can also react with O_3 to form N_2O_5 [121], as shown in reactions (6)–(8).

$$NO + O_3 \rightarrow NO_2 + O_2 \quad (6)$$

$$NO_2 + O_3 \rightarrow NO_3 + O_2 \quad (7)$$

$$NO_3 + NO_2 \leftrightarrow N_2O_5 \quad (8)$$

Among them, the wet and dry deposition of N_2O_5 and the uptake of N_2O_5 by aerosols are vital nighttime loss processes for NO_X. N_2O_5 is toxic and reacts readily with H_2O in the air, leading to nitric acid formation. Thus, this process also affects the environment and human health.

The reaction of OH radicals with NO and NO_2 is also essential in the troposphere, and the processes produce acids such as HONO and HNO_3, as shown in (9) and (10).

$$OH + NO \rightarrow HONO \quad (9)$$

$$OH + NO_2 \rightarrow HNO_3 \quad (10)$$

Then, HONO photolyzes and produces OH radicals with NO, as shown in reaction (11).

$$HONO + hv \rightarrow OH + NO \quad (11)$$

Due to the heterogeneous hydrolysis of NO_2 on the surface of aerosols and particulate matter, HONO formation can be observed during nighttime in urban areas. The HONO produced at night is rapidly photolyzed again after sunrise, leading to a rapid rise in OH radicals in the early morning, acting as an urban photochemical initiator [121]. Figure 6 shows the major NO_X reaction processes under "clean" tropospheric conditions.

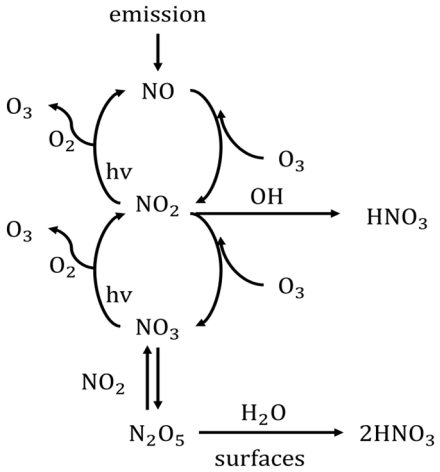


Figure 6. NO_X reactions involved in the troposphere.

In summary, there is a complicated relationship between the photochemical reactions of ozone and its precursors, VOCs and NO_X, which slightly complicated the reduction in ozone pollution. Additionally, some secondary oxidation products have lower vapor pressure and can attach to the pre-existing primary particulate matter through homogeneous nucleation or condensation, leading to SOA formation, thus leading to adverse environmental problems [121,122]. Therefore, understanding the chemical reaction mechanism of VOCs-NO_X-O_3 is one of the significant scientific challenges related to urban air pollution.

6.2. Relationship among the Vertical Distributions of VOCs, NO_X, and O_3

The vertical distribution characteristics of VOCs and NO_X show an overall negative trend with respect to the vertical distribution of O_3. Namely, VOCs and NO_X concentrations decrease with the increase in height, while O_3 concentrations increase [53,54,98,123]. It is mainly because VOCs and NO_X can generate O_3 in the atmosphere through a series of photochemical reactions (as mentioned in 4.1) after being emitted at the ground level. For example, Zhang et al. [98] used a tethered balloon to observe the vertical distribution of O_3 and its precursor VOCs in the lower 1000 m of the troposphere, at 50–350 m, 350–700 m, and 700–1000 m, in the suburbs of Shanghai, China. The results showed that the average hourly O_3 concentration was negatively correlated with the TVOC concentrations, with a correlation coefficient of -0.29 ($p < 0.05$) [98]. Wohrnschimmel et al. [55] measured ozone profiles between 0 and 1000 m above the ground. The result showed that the concentration of O_3 reached 60–70 ppb at the top of the surface layer and maintained these concentrations throughout the residual layer [55]. Tsai et al. [54] found that the O_3 concentration at 100–500 m was higher than the ground O_3 level, with a core up to 85 ppb at 300–500 m. The concentration tended to decrease with the increase in height when the altitude was up to 500 m [54]; this is because the concentration of VOC, as precursors of O_3, reduce at this altitude, resulting in weak O_3 production [123].

However, with a further increase in altitude, VOC and NO_X concentrations in the upper atmosphere gradually decrease, which leads to a net decrease in O_3 production. Therefore, when the altitude exceeds a specific range (generally above the PBL), the O_3 concentration also tends to decrease [123,124]. Yang et al. [125] divided the vertical distribution of O_3 into three layers based on the vertical distribution of NO_X. The first layer was from the surface to 200 m above the ground, with a high NO concentration, which prompts the conversion between O_3 and NO_2 (as shown in reaction (5)), making O_3 and NO_2 concentrations exhibit a relatively strong negative correlation [125]. The concentration of NO_2 gradually decreases with the increase in altitude, while the O_3 concentration increases. Especially at night and in the early morning, considering an altitude of up to 220 m, the concentration of O_3 is significantly higher than that at the ground level [126]. It should be noted that NO_X concentrations decrease faster at this altitude [123]. The second layer considered in the above-mentioned study was 200–1000 m above the ground, and the range of $d[O_3]/dt$ (daytime chemical production of O_3) was 10–40 $\mu g\ m^{-3}\ h^{-1}$. The maximum chemical production of O_3 occurred at 300 m. The third layer was outside the PBL height, where NO_X decreases rapidly. Additionally, the chemical production of O_3 is weak above the PBL [126], making the O_3 concentration tend to drop at this height. In addition, other factors such as weather conditions, prevailing wind direction, and pollution sources among different regions are also important factors that can affect the vertical distribution of VOCs, NO_X, and O_3 [90,127].

6.3. Effect of VOCs

The impact of VOCs on the atmospheric environment is mainly caused by tropospheric chemical processes leading to the production of O_3 and SOAs. The O_3 formation potential (OFP) and the SOA potential (SOAP) can describe the ability of O_3 and SOA formation of VOCs, thus providing a more direct indication of the extent of the VOCs' impact on the atmosphere.

The primary contributions to the OFP are aromatics, alkanes, and alkenes generated from the petrochemical industry and vehicle exhaust [89,98,126]. The OFP contributions of alkenes and aromatics change more significantly in the vertical direction. Alkenes increase with the increase in height, while aromatics show the opposite tendency. The concentration variation of alkanes is not significant in the vertical direction, mainly due to their relatively stable chemical properties [98,128]. The relatively small concentration changes in the vertical distribution of VOCs can lead to significant changes in the OFP. For example, Zhang et al. [98] found that the alkene contributions to TVOC concentrations were 8.41% and 12.12% at the surface and at 50–350 m, respectively, with less than 4% variation. In contrast, the contribution of alkenes to the OFP varied significantly, contributing 19% at the surface and then increasing rapidly to 49% at 50–350 m.

The contribution of the SOAP is mainly dominated by aromatics (up to 90%) [129,130]. Furthermore, this phenomenon exists at all altitudes [131]. One possible reason for these characteristics is that the high-carbon-content structures of aromatics can enter the particle phase more simply. In contrast, alkanes and alkenes are mostly low-carbon-content structure components whose oxidation products have higher saturation and vapor pressure and are less likely to enter the particulate phase to form SOAs [132]. However, the correlation among VOCs and the OFP, VOCs, and the SOAP may be insignificant. High TVOC concentrations may not necessarily contribute to a high OFP or SOAP [89,100].

As mentioned above, the primary contributions to the OFP and the SOAP are aromatics, alkanes, and alkenes. Among them, the contribution of aromatics to the SOAP is up to 90%. Aromatics, alkanes, and alkenes are mainly emitted by the petrochemical industry and through vehicle exhaust. Mastering these characteristics and emission sources of the OFP and the SOAP could help governments and other institutions to control O_3 and SOA pollution more effectively.

7. Research Prospects

The discussion above clearly shows that techniques based on towers/buildings, tethered balloons, aircrafts, and UAVs are widely applied in VOC sampling. Additionally, some studies of VOC photochemical reactions and VOC vertical distribution characteristics have also been conducted in recent years, and research in these directions will likely continue in the future. However, some details still need to be explored in the following aspects:

(1) Vertical sampling techniques for VOCs: Remote sensing and satellite technologies can monitor VOCs on the continental scale. However, it is not easy to obtain VOC vertical profiles. Thus, advanced sampling techniques must be explored to overcome the high cost, high risk, insufficient spatial scale, and other limitations of the current techniques.

(2) Vertical distribution characteristics of VOCs: Comparisons between VOC vertical distribution characteristics in different seasons and regions are incredibly lacking, and the explanations for the VOC vertical distribution characteristics are insufficient in current studies.

(3) Vertical distribution models of VOCs: Current VOCs dispersion models are mainly comprehensive models for simulating various pollutants, such as SO_2 and NO_X, with result accuracy limitations when facing different environments. Moreover, most of them are focused on ground-level simulations, while a specialized VOC vertical distribution model is highly lacking. In addition, the atmospheric environmental problems (e.g., OFP and SOAP) caused by VOC emissions should also be explored deeply.

(4) Effects caused by VOCs: Although research on VOC atmospheric chemistry has developed, the reaction rate constants and reaction mechanism of organic peroxides $R\dot{O}_2$ with NO and NO_2 radicals need to be further investigated.

(5) Sources of VOCs: Previous studies have generally focused on sources of VOCs near the ground level. Research on VOC sources in the vertical direction is extremely lacking. Additionally, a considerable research gap exists in studying VOC sources using PMF at different heights.

Author Contributions: Conceptualization, D.C., J.Z. and Y.X.; methodology, J.Z. and Y.X.; validation, J.Z. and Y.X.; formal analysis, Y.X.; investigation, Y.X., J.X., W.W. and M.W.; resources, D.C., J.Z., M.L. and W.Z.; data curation, J.Z.; writing—original draft preparation, J.Z. and Y.X.; writing—review and editing, J.Z. and Y.X..; supervision, D.C. and J.Z.; project administration, D.C. and J.Z.; funding acquisition, J.Z. All authors have read and agreed to the published version of the manuscript.

Funding: This research was funded by Fundamental Research Funds for the Central Universities (3122021059), National Natural Science Foundation of China (21973111, 61378048), and National Key R&D Program of China (2018YFF01011700).

Institutional Review Board Statement: Not applicable.

Informed Consent Statement: Not applicable.

Data Availability Statement: Not applicable.

Conflicts of Interest: The authors declare no conflict of interest. The funders had no role in the design of the study; in the collection, analyses, or interpretation of data; in the writing of the manuscript; or in the decision to publish the results.

References

1. Haick, H.; Broza, Y.Y.; Mochalski, P.; Ruzsanyi, V.; Amann, A. Assessment, origin, and implementation of breath volatile cancer markers. *Chem. Soc. Rev.* **2014**, *43*, 1423–1449. [CrossRef]
2. Wu, S.; Tang, G.Q.; Wang, Y.H.; Mai, R.; Yao, D.; Kang, Y.Y.; Wang, Q.L.; Wang, Y.S. Vertical Evolution of Boundary Layer Volatile Organic Compounds in Summer over the North China Plain and the Differences with Winter. *Adv. Atmos. Sci.* **2021**, *38*, 1165–1176. [CrossRef]
3. Wang, W.N.; Cheng, T.H.; Gu, X.F.; Chen, H.; Guo, H.; Wang, Y.; Bao, F.W.; Shi, S.Y.; Xu, B.R.; Zuo, X.; et al. Assessing Spatial and Temporal Patterns of Observed Ground-level Ozone in China. *Sci. Rep.* **2017**, *7*, 3651. [CrossRef] [PubMed]
4. Harrison, R.M.; Yin, J.X. Particulate matter in the atmosphere: Which particle properties are important for its effects on health? *Sci. Total Environ.* **2000**, *249*, 85–101. [CrossRef] [PubMed]
5. Velasco, E.; Marquez, C.; Bueno, E.; Bernabe, R.M.; Sanchez, A.; Fentanes, O.; Wohrnschimmel, H.; Cardenas, B.; Kamilla, A.; Wakamatsu, S.; et al. Vertical distribution of ozone and VOCs in the low boundary layer of Mexico City. *Atmos. Chem. Phys.* **2008**, *8*, 3061–3079. [CrossRef]
6. Geng, C.M.; Wang, J.; Yin, B.H.; Zhao, R.J.; Li, P.; Yang, W.; Xiao, Z.M.; Li, S.J.; Li, K.W.; Bai, Z.P. Vertical distribution of volatile organic compounds conducted by tethered balloon in the Beijing-Tianjin-Hebei region of China. *J. Environ. Sci.* **2020**, *95*, 121–129. [CrossRef]
7. Zhang, K.; Zhou, L.; Fu, Q.Y.; Yan, L.; Bian, Q.G.; Wang, D.F.; Xiu, G.L. Vertical distribution of ozone over Shanghai during late spring: A balloon-borne observation. *Atmos. Environ.* **2019**, *208*, 48–60. [CrossRef]
8. Wu, R.R.; Xie, S.D. Spatial Distribution of Ozone Formation in China Derived from Emissions of Speciated Volatile Organic Compounds. *Environ. Sci. Technol.* **2017**, *51*, 2574–2583. [CrossRef]
9. Holmes, N.S.; Morawska, L. A review of dispersion modelling and its application to the dispersion of particles: An overview of different dispersion models available. *Atmos. Environ.* **2006**, *40*, 5902–5928. [CrossRef]
10. Qi, Y.; Shen, L.; Zhang, J.; Yao, J.; Lu, R.; Miyakoshi, T. Species and release characteristics of VOCs in furniture coating process. *Environ. Pollut.* **2019**, *245*, 810–819. [CrossRef]
11. Sun, C.; Zhao, L.; Chen, X.; Nie, L.; Shi, A.; Bai, H.; Li, G. A comprehensive study of volatile organic compounds from the actual emission of Chinese cooking. *Environ. Sci. Pollut. Res.* **2022**, *29*, 53821–53830. [CrossRef]
12. Zhong, Z.; Sha, Q.e.; Zheng, J.; Yuan, Z.; Gao, Z.; Ou, J.; Zheng, Z.; Li, C.; Huang, Z. Sector-based VOCs emission factors and source profiles for the surface coating industry in the Pearl River Delta region of China. *Sci. Total Environ.* **2017**, *583*, 19–28. [CrossRef] [PubMed]
13. Sexton, K.; Westberg, H. Nonmethane hydrocarbon composition of urban and rural atmospheres. *Atmos. Environ.* **1984**, *18*, 1125–1132. [CrossRef]
14. Wei, W.; Wang, S.X.; Hao, J.M.; Cheng, S.Y. Trends of chemical speciation profiles of anthropogenic volatile organic compounds emissions in China, 2005–2020. *Front. Environ. Sci. Eng.* **2014**, *8*, 27–41. [CrossRef]
15. Zheng, C.; Shen, J.; Zhang, Y.; Zhu, X.; Wu, X.; Chen, L.; Gao, X. Atmospheric Emission Characteristics and Control Policies of Anthropogenic VOCs from Industrial Sources in Yangtze River Delta Region, China. *Aerosol Air Qual. Res.* **2017**, *17*, 2263–2275. [CrossRef]
16. Mao, T.; Wang, Y.S.; Xu, H.H.; Jiang, J.; Wu, F.K.; Xu, X.B. A study of the atmospheric VOCs of Mount Tai in June 2006. *Atmos. Environ.* **2009**, *43*, 2503–2508. [CrossRef]
17. Zhang, J.K.; Sun, Y.; Wu, F.K.; Sun, J.; Wang, Y.S. The characteristics, seasonal variation and source apportionment of VOCs at Gongga Mountain, China. *Atmos. Environ.* **2014**, *88*, 297–305. [CrossRef]

18. Mao, T.; Wang, Y.S.; Jiang, J.; Wu, F.K.; Wang, M.X. The vertical distributions of VOCs in the atmosphere of Beijing in autumn. *Sci. Total Environ.* **2008**, *390*, 97–108. [CrossRef]
19. Yang, J.J.; Liu, C.C.; Chen, W.H.; Yuan, C.S.; Lin, C. Assessing the altitude effect on distributions of volatile organic compounds from different sources by principal component analysis. *Environ. Sci. Process. Impacts* **2013**, *15*, 972–985. [CrossRef]
20. Gupta, S.; Gadi, R.; Sharma, S.K.; Mandal, T.K. Characterization and source apportionment of organic compounds in PM10 using PCA and PMF at a traffic hotspot of Delhi. *Sustain. Cities Soc.* **2018**, *39*, 52–67. [CrossRef]
21. Ling, Z.H.; Guo, H.; Cheng, H.R.; Yu, Y.F. Sources of ambient volatile organic compounds and their contributions to photochemical ozone formation at a site in the Pearl River Delta, southern China. *Environ. Pollut.* **2011**, *159*, 2310–2319. [CrossRef] [PubMed]
22. Chen, W.T.; Shao, M.; Lu, S.H.; Wang, M.; Zeng, L.M.; Yuan, B.; Liu, Y. Understanding primary and secondary sources of ambient carbonyl compounds in Beijing using the PMF model. *Atmos. Chem. Phys.* **2014**, *14*, 3047–3062. [CrossRef]
23. Chan, Y.-c.; Hawas, O.; Hawker, D.; Vowles, P.; Cohen, D.D.; Stelcer, E.; Simpson, R.; Golding, G.; Christensen, E. Using multiple type composition data and wind data in PMF analysis to apportion and locate sources of air pollutants. *Atmos. Environ.* **2011**, *45*, 439–449. [CrossRef]
24. Yuan, B.; Shao, M.; de Gouw, J.; Parrish, D.D.; Lu, S.; Wang, M.; Zeng, L.; Zhang, Q.; Song, Y.; Zhang, J.; et al. Volatile organic compounds (VOCs) in urban air: How chemistry affects the interpretation of positive matrix factorization (PMF) analysis. *J. Geophys. Res. Atmos.* **2012**, *117*, 3091–3108. [CrossRef]
25. Masiol, M.; Harrison, R.M. Aircraft engine exhaust emissions and other airport-related contributions to ambient air pollution: A review. *Atmos. Environ.* **2014**, *95*, 409–455. [CrossRef]
26. Pecorari, E.; Mantovani, A.; Franceschini, C.; Bassano, D.; Palmeri, L.; Rampazzo, G. Analysis of the effects of meteorology on aircraft exhaust dispersion and deposition using a Lagrangian particle model. *Sci. Total Environ.* **2016**, *541*, 839–856. [CrossRef]
27. Beyersdorf, A.J.; Thornhill, K.L.; Winstead, E.L.; Ziemba, L.D.; Blake, D.R.; Timko, M.T.; Anderson, B.E. Power-dependent speciation of volatile organic compounds in aircraft exhaust. *Atmos. Environ.* **2012**, *61*, 275–282. [CrossRef]
28. Kumar, A.; Víden, I. Volatile Organic Compounds: Sampling Methods and Their Worldwide Profile in Ambient Air. *Environ. Monit. Assess.* **2007**, *131*, 301–321. [CrossRef]
29. Krol, S.; Zabiegala, B.; Namiesnik, J. Monitoring VOCs in atmospheric air II. Sample collection and preparation. *TrAC Trends Anal. Chem.* **2010**, *29*, 1101–1112. [CrossRef]
30. Toscano, P.; Gioli, B.; Dugheri, S.; Salvini, A.; Matese, A.; Bonacchi, A.; Zaldei, A.; Cupelli, V.; Miglietta, F. Locating industrial VOC sources with aircraft observations. *Environ. Pollut.* **2011**, *159*, 1174–1182. [CrossRef]
31. Liu, Y.; Feng, X.; Lawless, D. Separation of gasoline vapor from nitrogen by hollow fiber composite membranes for VOC emission control. *J. Membr. Sci.* **2006**, *271*, 114–124. [CrossRef]
32. Kim, Y.-H.; Kim, K.-H.; Jo, S.-H.; Jeon, E.-C.; Sohn, J.R.; Parker, D.B. Comparison of storage stability of odorous VOCs in polyester aluminum and polyvinyl fluoride Tedlar® bags. *Anal. Chim. Acta* **2012**, *712*, 162–167. [CrossRef] [PubMed]
33. Zhu, W.; Koziel, J.A.; Cai, L.; Wright, D.; Kuhrt, F. Testing odorants recovery from a novel metallized fluorinated ethylene propylene gas sampling bag. *J. Air Waste Manag. Assoc.* **2015**, *65*, 1434–1445. [CrossRef] [PubMed]
34. Fleming, L.T.; Weltman, R.; Yadav, A.; Edwards, R.D.; Arora, N.K.; Pillarisetti, A.; Meinardi, S.; Smith, K.R.; Blake, D.R.; Nizkorodov, S.A. Emissions from village cookstoves in Haryana, India, and their potential impacts on air quality. *Atmos. Chem. Phys.* **2018**, *18*, 15169–15182. [CrossRef]
35. Cariou, S.; Guillot, J.M. Double-layer Tedlar bags: A means to limit humidity evolution of air samples and to dry humid air samples. *Anal. Bioanal. Chem.* **2006**, *384*, 468–474. [CrossRef]
36. Hien, V.T.D.; Lin, C.; Thanh, V.C.; Oanh, N.T.K.; Thanh, B.X.; Weng, C.E.; Yuan, C.S.; Rene, E.R. An overview of the development of vertical sampling technologies for ambient volatile organic compounds (VOCs). *J. Environ. Manage.* **2019**, *247*, 401–412. [CrossRef]
37. Wang, D.K.W.; Austin, C.C. Determination of complex mixtures of volatile organic compounds in ambient air: An overview. *Anal. Bioanal. Chem.* **2006**, *386*, 1089–1098. [CrossRef]
38. Dobrzynska, E.; Posniak, M.; Szewczynska, M.; Buszewski, B. Chlorinated Volatile Organic Compounds-Old, However, Actual Analytical and Toxicological Problem. *Crit. Rev. Anal. Chem.* **2010**, *40*, 41–57. [CrossRef]
39. Wang, D.K.W.; Austin, C.C. Determination of complex mixtures of volatile organic compounds in ambient air: Canister methodology. *Anal. Bioanal. Chem.* **2006**, *386*, 1099–1120. [CrossRef]
40. Ras, M.R.; Borrull, F.; Marce, R.M. Sampling and preconcentration techniques for determination of volatile organic compounds in air samples. *TrAC Trends Anal. Chem.* **2009**, *28*, 347–361. [CrossRef]
41. Mangani, G.; Berloni, A.; Maione, M. "Cold" solid-phase microextraction method for the determination of volatile halocarbons present in the atmosphere at ultra-trace levels. *J. Chromatogr. A* **2003**, *988*, 167–175. [CrossRef] [PubMed]
42. Koziel, J.A.; Pawliszyn, J. Air sampling and analysis of volatile organic compounds with solid phase microextraction. *J. Air Waste Manage. Assoc.* **2001**, *51*, 173–184. [CrossRef] [PubMed]
43. Ras, M.R.; Marce, R.M.; Borrull, F. Solid-phase microextraction-Gas chromatography to determine volatile organic sulfur compounds in the air at sewage treatment plants. *Talanta* **2008**, *77*, 774–778. [CrossRef]
44. Mochalski, P.; King, J.; Unterkofler, K.; Amann, A. Stability of selected volatile breath constituents in Tedlar, Kynar and Flexfilm sampling bags. *Analyst* **2013**, *138*, 1405–1418. [CrossRef]

45. Herrington, J.S. Storage stability of 66 volatile organic compounds (VOCs) in silicon-lined air canisters for 30 days. *Appl. Note EVAN* **2015**. Available online: https://www.restek.com/row/technical-literature-library/articles/storage-stability-of-66-volatile-organic-compounds-VOCs-in-silicon-lined-air-canisters-for-30-days/ (accessed on 19 October 2022).
46. Heo, G.S.; Lee, J.-H.; Kim, D.W.; Lee, D.W. Comparison of analytical methods for ozone precursors using adsorption tube and canister. *Microchem. J.* **2001**, *70*, 275–283. [CrossRef]
47. Sigma, S. *SPME for GC Analysis: Getting started with Solid Phase Microextraction*; Merck: Darmstadt, Germany, 2018. Available online: https://www.sigmaaldrich.com/deepweb/assets/sigmaaldrich/marketing/global/documents/635/441/solid-phase-microextraction-for-gc-ms.pdf (accessed on 19 October 2022).
48. Woolfenden, E. Sorbent-based sampling methods for volatile and semi-volatile organic compounds in air: Part 1: Sorbent-based air monitoring options. *J. Chromatogr. A* **2010**, *1217*, 2674–2684. [CrossRef]
49. Kaser, L.; Peron, A.; Graus, M.; Striednig, M.; Wohlfahrt, G.; Juráň, S.; Karl, T. Interannual variability of terpenoid emissions in an alpine city. *Atmos. Chem. Phys.* **2022**, *22*, 5603–5618. [CrossRef]
50. Li, X.B.; Yuan, B.; Wang, S.; Wang, C.; Lan, J.; Liu, Z.; Song, Y.; He, X.; Huangfu, Y.; Pei, C.; et al. Variations and sources of volatile organic compounds (VOCs) in urban region: Insights from measurements on a tall tower. *Atmos. Chem. Phys.* **2022**, *22*, 10567–10587. [CrossRef]
51. Zhang, H.; Zhang, Y.; Huang, Z.; Acton, W.J.F.; Wang, Z.; Nemitz, E.; Langford, B.; Mullinger, N.; Davison, B.; Shi, Z.; et al. Vertical profiles of biogenic volatile organic compounds as observed online at a tower in Beijing. *J. Environ. Sci.* **2020**, *95*, 33–42. [CrossRef]
52. Ieda, T.; Kitamori, Y.; Mochida, M.; Hirata, R.; Hirano, T.; Inukai, K.; Fujinuma, Y.; Kawamura, K. Diurnal variations and vertical gradients of biogenic volatile and semi-volatile organic compounds at the Tomakomai larch forest station in Japan. *Tellus B* **2006**, *58*, 177–186. [CrossRef]
53. Sangiorgi, G.; Ferrero, L.; Perrone, M.G.; Bolzacchini, E.; Duane, M.; Larsen, B.R. Vertical distribution of hydrocarbons in the low troposphere below and above the mixing height: Tethered balloon measurements in Milan, Italy. *Environ. Pollut.* **2011**, *159*, 3545–3552. [CrossRef] [PubMed]
54. Tsai, H.H.; Liu, Y.F.; Yuan, C.S.; Chen, W.H.; Lin, Y.C.; Hung, C.H.; Lin, C.; Jen, Y.H.; Ie, I.R.; Yang, H.Y. Vertical Profile and Spatial Distribution of Ozone and Its Precursors at the Inland and Offshore of an Industrial City. *Aerosol Air Qual. Res.* **2012**, *12*, 911–922. [CrossRef]
55. Wohrnschimmel, H.; Marquez, C.; Mugica, V.; Stahel, W.A.; Staehelin, J.; Cardenas, B.; Blanco, S. Vertical profiles and receptor modeling of volatile organic compounds over Southeastern Mexico City. *Atmos. Environ.* **2006**, *40*, 5125–5136. [CrossRef]
56. Helmig, D.; Balsley, B.; Davis, K.; Kuck, L.R.; Jensen, M.; Bognar, J.; Smith, T.; Arrieta, R.V.; Rodriguez, R.; Birks, J.W. Vertical profiling and determination of landscape fluxes of biogenic nonmethane hydrocarbons within the planetary boundary layer in the Peruvian Amazon. *J. Geophys. Res. D Atmos.* **1998**, *103*, 25519–25532. [CrossRef]
57. Permar, W.; Wang, Q.; Selimovic, V.; Wielgasz, C.; Yokelson, R.J.; Hornbrook, R.S.; Hills, A.J.; Apel, E.C.; Ku, I.T.; Zhou, Y.; et al. Emissions of Trace Organic Gases From Western U.S. Wildfires Based on WE-CAN Aircraft Measurements. *J. Geophys. Res. Atmos.* **2021**, *126*, e2020JD033838. [CrossRef]
58. Koss, A.; Yuan, B.; Warneke, C.; Gilman, J.B.; Lerner, B.M.; Veres, P.R.; Peischl, J.; Eilerman, S.; Wild, R.; Brown, S.S.; et al. Observations of VOC emissions and photochemical products over US oil- and gas-producing regions using high-resolution H3O+ CIMS (PTR-ToF-MS). *Atmos. Meas. Technol.* **2017**, *10*, 2941–2968. [CrossRef]
59. Veres, P.R.; Faber, P.; Drewnick, F.; Lelieveld, J.; Williams, J. Anthropogenic sources of VOC in a football stadium: Assessing human emissions in the atmosphere. *Atmos. Environ.* **2013**, *77*, 1052–1059. [CrossRef]
60. Flocas, H.A.; Assimakopoulos, V.D.; Helmis, C.G.; Gusten, H. VOC and O3 distributions over the densely populated area of greater Athens, Greece. *J. Appl. Meteorol.* **2003**, *42*, 1799–1810. [CrossRef]
61. Xue, L.K.; Wang, T.; Simpson, I.J.; Ding, A.J.; Gao, J.; Blake, D.R.; Wang, X.Z.; Wang, W.X.; Lei, H.C.; Jing, D.Z. Vertical distributions of non-methane hydrocarbons and halocarbons in the lower troposphere over northeast China. *Atmos. Environ.* **2011**, *45*, 6501–6509. [CrossRef]
62. Koßmann, M.; Vogel, H.; Vogel, B.; Vögtlin, R.; Corsmeier, U.; Fiedler, F.; Klemm, O.; Schlager, H. The composition and vertical distribution of volatile organic compounds in southwestern Germany, eastern France and northern Switzerland during the TRACT campaign in September 1992. *Phys. Chem. Earth.* **1996**, *21*, 429–433. [CrossRef]
63. Wespes, C.; Emmons, L.; Edwards, D.P.; Hannigan, J.; Hurtmans, D.; Saunois, M.; Coheur, P.F.; Clerbaux, C.; Coffey, M.T.; Batchelor, R.L.; et al. Analysis of ozone and nitric acid in spring and summer Arctic pollution using aircraft, ground-based, satellite observations and MOZART-4 model: Source attribution and partitioning. *Atmos. Chem. Phys.* **2012**, *12*, 237–259. [CrossRef]
64. Duncan, B.N.; Prados, A.I.; Lamsal, L.N.; Liu, Y.; Streets, D.G.; Gupta, P.; Hilsenrath, E.; Kahn, R.; Nielsen, J.E.; Beyersdorf, A.J.; et al. Satellite data of atmospheric pollution for U.S. air quality applications: Examples of applications, summary of data end-user resources, answers to FAQs, and common mistakes to avoid. *Atmos. Environ.* **2014**, *94*, 647–662. [CrossRef]
65. Cao, H.S.; Fu, T.M.; Zhang, L.; Henze, D.K.; Miller, C.C.; Lerot, C.; Abad, G.G.; De Smedt, I.; Zhang, Q.; Van Roozendael, M.; et al. Adjoint inversion of Chinese non-methane volatile organic compound emissions using space-based observations of formaldehyde and glyoxal. *Atmos. Chem. Phys.* **2018**, *18*, 15017–15046. [CrossRef]

66. Zeb, N.; Khokhar, M.F.; Pozzer, A.; Khan, S.A. Exploring the temporal trends and seasonal behaviour of tropospheric trace gases over Pakistan by exploiting satellite observations. *Atmos. Environ.* **2019**, *198*, 279–290. [CrossRef]
67. Kota, H.; Guo, H.; Myllyvirta, L.; Hu, J.L.; Sahu, S.K.; Garaga, R.; Ying, Q.; Gao, A.F.; Dahiya, S.; Wang, Y.; et al. Year-long simulation of gaseous and particulate air pollutants in India. *Atmos. Environ.* **2018**, *180*, 244–255. [CrossRef]
68. Ul-Haq, Z.; Ramzan, Z.; Tariq, S.; Batool, S.A.; Ali, M.; Sami, J. Comparison of total ozone column observations from space-borne Ozone Monitoring Instrument with ground-based Dobson Ozone Spectrophotometer measurements at an urban location in Indo-Gangetic Basin. *Int. J. Remote Sens.* **2018**, *39*, 544–564. [CrossRef]
69. Jin, X.M.; Fiore, A.; Boersma, K.F.; De Smedt, I.; Valin, L. Inferring Changes in Summertime Surface Ozone-NOx-VOC Chemistry over US Urban Areas from Two Decades of Satellite and Ground-Based Observations. *Environ. Sci. Technol.* **2020**, *54*, 6518–6529. [CrossRef]
70. McKinney, K.A.; Wang, D.; Ye, J.H.; de Fouchier, J.B.; Guimaraes, P.C.; Batista, C.E.; Souza, R.A.F.; Alves, E.G.; Gu, D.; Guenther, A.B.; et al. A sampler for atmospheric volatile organic compounds by copter unmanned aerial vehicles. *Atmos. Meas. Technol.* **2019**, *12*, 3123–3135. [CrossRef]
71. Peng, Z.R.; Wang, D.S.; Wang, Z.Y.; Gao, Y.; Lu, S.J. A study of vertical distribution patterns of PM2.5 concentrations based on ambient monitoring with unmanned aerial vehicles: A case in Hangzhou, China. *Atmos. Environ.* **2015**, *123*, 357–369. [CrossRef]
72. Yu, F.J.; Liu, Y.F.; Fan, L.Q.; Li, L.H.; Han, Y.; Chen, G. Design and implementation of atmospheric multi-parameter sensor for UAV-based aerosol distribution detection. *Sens. Rev.* **2017**, *37*, 196–210. [CrossRef]
73. Li, X.B.; Wang, D.S.; Lu, Q.C.; Peng, Z.R.; Lu, S.J.; Li, B.; Li, C. Three-dimensional investigation of ozone pollution in the lower troposphere using an unmanned aerial vehicle platform. *Environ. Pollut.* **2017**, *224*, 107–116. [CrossRef]
74. Klemas, V.V. Coastal and Environmental Remote Sensing from Unmanned Aerial Vehicles: An Overview. *J. Coast. Res.* **2015**, *31*, 1260–1267. [CrossRef]
75. Neumann, P.P.; Bennetts, V.H.; Lilienthal, A.J.; Bartholmai, M.; Schiller, J.H. Gas source localization with a micro-drone using bio-inspired and particle filter-based algorithms. *Adv. Rob.* **2013**, *27*, 725–738. [CrossRef]
76. Brady, J.M.; Stokes, M.D.; Bonnardel, J.; Bertram, T.H. Characterization of a Quadrotor Unmanned Aircraft System for Aerosol-Particle-Concentration Measurements. *Environ. Sci. Technol.* **2016**, *50*, 1376–1383. [CrossRef] [PubMed]
77. Andrews, S.J.; Hackenberg, S.C.; Carpenter, L.J. Technical Note: A fully automated purge and trap GC-MS system for quantification of volatile organic compound (VOC) fluxes between the ocean and atmosphere. *Ocean Sci.* **2015**, *11*, 313–321. [CrossRef]
78. Han, C.; Liu, R.; Luo, H.; Li, G.; Ma, S.; Chen, J.; An, T. Pollution profiles of volatile organic compounds from different urban functional areas in Guangzhou China based on GC/MS and PTR-TOF-MS: Atmospheric environmental implications. *Atmos. Environ.* **2019**, *214*, 116843. [CrossRef]
79. Vinaixa, M.; Schymanski, E.L.; Neumann, S.; Navarro, M.; Salek, R.M.; Yanes, O. Mass spectral databases for LC/MS- and GC/MS-based metabolomics: State of the field and future prospects. *TrAC Trends Anal. Chem.* **2016**, *78*, 23–35. [CrossRef]
80. Warneke, C.; de Gouw, J.A.; Kuster, W.C.; Goldan, P.D.; Fall, R. Validation of Atmospheric VOC Measurements by Proton-Transfer-Reaction Mass Spectrometry Using a Gas-Chromatographic Preseparation Method. *Environ. Sci. Technol.* **2003**, *37*, 2494–2501. [CrossRef] [PubMed]
81. Wieland, F.; Gloess, A.N.; Keller, M.; Wetzel, A.; Schenker, S.; Yeretzian, C. Online monitoring of coffee roasting by proton transfer reaction time-of-flight mass spectrometry (PTR-ToF-MS): Towards a real-time process control for a consistent roast profile. *Anal. Bioanal. Chem.* **2012**, *402*, 2531–2543. [CrossRef] [PubMed]
82. Pleil, J.D.; Hansel, A.; Beauchamp, J. Advances in proton transfer reaction mass spectrometry (PTR-MS): Applications in exhaled breath analysis, food science, and atmospheric chemistry. *J. Breath Res.* **2019**, *13*, 039002. [CrossRef]
83. Lin, C.C.; Lin, C.; Hsieh, L.T.; Chen, C.Y.; Wang, J.P. Vertical and Diurnal Characterization of Volatile Organic Compounds in Ambient Air in Urban Areas. *J. Air Waste Manage. Assoc.* **2011**, *61*, 714–720. [CrossRef] [PubMed]
84. Jo, W.-K.; Kim, K.-Y. Vertical variability of volatile organic compound (VOC) levels in ambient air of high-rise apartment buildings with and without occurrence of surface inversion. *Atmos. Environ.* **2002**, *36*, 5645–5652. [CrossRef]
85. Noe, S.M.; Hüve, K.; Niinemets, Ü.; Copolovici, L. Seasonal variation in vertical volatile compounds air concentrations within a remote hemiboreal mixed forest. *Atmos. Chem. Phys.* **2012**, *12*, 3909–3926. [CrossRef]
86. Vierling, L.A.; Fersdahl, M.; Chen, X.; Li, Z.; Zimmerman, P. The Short Wave Aerostat-Mounted Imager (SWAMI): A novel platform for acquiring remotely sensed data from a tethered balloon. *Remote Sens. Environ.* **2006**, *103*, 255–264. [CrossRef]
87. Liu, K.; Quan, J.; Mu, Y.; Zhang, Q.; Liu, J.; Gao, Y.; Chen, P.; Zhao, D.; Tian, H. Aircraft measurements of BTEX compounds around Beijing city. *Atmos. Environ.* **2013**, *73*, 11–15. [CrossRef]
88. Mak, J.E.; Su, L.; Guenther, A.; Karl, T. A novel Whole Air Sample Profiler (WASP) for the quantification of volatile organic compounds in the boundary layer. *Atmos. Meas. Technol.* **2013**, *6*, 2703–2712. [CrossRef]
89. Vo, T.D.H.; Lin, C.T.; Weng, C.E.; Yuan, C.S.; Lee, C.W.; Hung, C.H.; Bui, X.T.; Lo, K.C.; Lin, J.X. Vertical stratification of volatile organic compounds and their photochemical product formation potential in an industrial urban area. *J. Environ. Manag.* **2018**, *217*, 327–336. [CrossRef] [PubMed]
90. Whitehead, K.; Hugenholtz, C.H. Remote sensing of the environment with small unmanned aircraft systems (UASs), part 1: A review of progress and challenges. *J. Unmanned Veh. Syst.* **2014**, *02*, 69–85. [CrossRef]
91. Chang, C.-C.; Wang, J.-L.; Chang, C.-Y.; Liang, M.-C.; Lin, M.-R. Development of a multicopter-carried whole air sampling apparatus and its applications in environmental studies. *Chemosphere* **2016**, *144*, 484–492. [CrossRef]

92. Seibert, P.; Beyrich, F.; Gryning, S.-E.; Joffre, S.; Rasmussen, A.; Tercier, P. Review and intercomparison of operational methods for the determination of the mixing height. *Atmos. Environ.* **2000**, *34*, 1001–1027. [CrossRef]
93. Xiong, Y.; Bari, M.A.; Xing, Z.Y.; Du, K. Ambient volatile organic compounds (VOCs) in two coastal cities in western Canada: Spatiotemporal variation, source apportionment, and health risk assessment. *Sci. Total Environ.* **2020**, *706*, 135970. [CrossRef] [PubMed]
94. Na, K.; Kim, Y.P. Seasonal characteristics of ambient volatile organic compounds in Seoul, Korea. *Atmos. Environ.* **2001**, *35*, 2603–2614. [CrossRef]
95. Ruiz-Jimenez, J.; Lan, H.Z.; Leleev, Y.; Hartonen, K.; Riekkola, M.L. Comparison of multiple calibration approaches for the determination of volatile organic compounds in air samples by solid phase microextraction Arrow and in-tube extraction. *J. Chromatogr. A* **2020**, *1616*, 460825. [CrossRef] [PubMed]
96. Field, R.A.; Goldstone, M.E.; Lester, J.N.; Perry, R. The sources and behaviour of tropospheric anthropogenic volatile hydrocarbons. *Atmos. Environment. Part A. Gen. Top.* **1992**, *26*, 2983–2996. [CrossRef]
97. Jin, X.M.; Fiore, A.; Murray, L.T.; Valin, L.C.; Lamsal, L.N.; Duncan, B.; Folkert Boersma, K.; De Smedt, I.; Abad, G.G.; Chance, K.; et al. Evaluating a Space-Based Indicator of Surface Ozone-NOx-VOC Sensitivity Over Midlatitude Source Regions and Application to Decadal Trends. *J. Geophys. Res. Atmos.* **2017**, *122*, 410–439. [CrossRef]
98. Zhang, K.; Xiu, G.L.; Zhou, L.; Bian, Q.G.; Duan, Y.S.; Fei, D.N.; Wang, D.F.; Fu, Q.Y. Vertical distribution of volatile organic compounds within the lower troposphere in late spring of Shanghai. *Atmos. Environ.* **2018**, *186*, 150–157. [CrossRef]
99. Cabañas, B.; Villanueva, F.; Martín, P.; Baeza, M.T.; Salgado, S.; Jiménez, E. Study of reaction processes of furan and some furan derivatives initiated by Cl atoms. *Atmos. Environ.* **2005**, *39*, 1935–1944. [CrossRef]
100. Liu, Y.H.; Wang, H.L.; Jing, S.A.; Zhou, M.; Lou, S.R.; Qu, K.; Qiu, W.Y.; Wang, Q.; Li, S.L.; Gao, Y.Q.; et al. Vertical Profiles of Volatile Organic Compounds in Suburban Shanghai. *Adv. Atmos. Sci.* **2021**, *38*, 1177–1187. [CrossRef]
101. Das, M.; Aneja, V.P.; Kang, D. Vertical distribution of VOCs and ozone observed in suburban North Carolina. *IJGEnvI* **2006**, *6*, 149–172. [CrossRef]
102. Brook, J.R.; Makar, P.A.; Sills, D.M.L.; Hayden, K.L.; McLaren, R. Exploring the nature of air quality over southwestern Ontario: Main findings from the Border Air Quality and Meteorology Study. *Atmos. Chem. Phys.* **2013**, *13*, 10461–10482. [CrossRef]
103. Liu, K.Y.; Wang, Z.F.; Hsiao, L.F. A modeling of the sea breeze and its impacts on ozone distribution in northern Taiwan. *Env. Model. Softw.* **2002**, *17*, 21–27. [CrossRef]
104. Jeon, W.B.; Lee, S.H.; Lee, H.; Park, C.; Kim, D.H.; Park, S.Y. A study on high ozone formation mechanism associated with change of NOx/VOCs ratio at a rural area in the Korean Peninsula. *Atmos. Environ.* **2014**, *89*, 10–21. [CrossRef]
105. Talbot, C.; Augustin, P.; Leroy, C.; Willart, V.; Delbarre, H.; Khomenko, G. Impact of a sea breeze on the boundary-layer dynamics and the atmospheric stratification in a coastal area of the North Sea. *Bound. Layer Meteorol.* **2007**, *125*, 133–154. [CrossRef]
106. Hanna, S.R.; Egan, B.A.; Purdum, J. A review of dispersion modelling and, AERMOD, and ISC3 dispersion models with the OPTEX, Duke Forest, Kincaid, Indianapolis and Lovett field datasets. *Int. J. Environ. Pollut.* **2001**, *16*, 301–314. [CrossRef]
107. Kumar, A.; Jimenez, R.; Belalcazar, L.C.; Rojas, N.Y. Application of WRF-Chem Model to Simulate PM10 Concentration over Bogota. *Aerosol Air Qual. Res.* **2016**, *16*, 1206–1221. [CrossRef]
108. Dennis, R.L.; Byun, D.W.; Novak, J.H.; Galluppi, K.J.; Coats, C.J.; Vouk, M.A. The next generation of integrated air quality modeling: EPA's models-3. *Atmos. Environ.* **1996**, *30*, 1925–1938. [CrossRef]
109. Byun, D.; Schere, K.L. Review of the governing equations, computational algorithms, and other components of the models-3 Community Multiscale Air Quality (CMAQ) modeling system. *Appl. Mech. Rev.* **2006**, *59*, 51–77. [CrossRef]
110. Sokhi, R.S.; San Jose, R.; Kitwiroon, N.; Fragkou, E.; Perez, J.L.; Middleton, D.R. Sexton. *Environ. Model. Softw.* **2006**, *21*, 566–576. [CrossRef]
111. Kwak, B.K.; Kim, J.H.; Park, H.S.; Kim, N.G.; Choi, K.; Yi, J. A GIS-based national emission inventory of major VOCs and risk assessment modeling: Part II—Quantitative verification and risk assessment using an air dispersion model. *Korean J. Chem. Eng.* **2010**, *27*, 121–128. [CrossRef]
112. Grell, G.A.; Peckham, S.E.; Schmitz, R.; McKeen, S.A.; Frost, G.; Skamarock, W.C.; Eder, B. Fully coupled "online" chemistry within the WRF model. *Atmos. Environ.* **2005**, *39*, 6957–6975. [CrossRef]
113. Chapman, E.G.; Gustafson, W.I., Jr.; Easter, R.C.; Barnard, J.C.; Ghan, S.J.; Pekour, M.S.; Fast, J.D. Coupling aerosol-cloud-radiative processes in the WRF-Chem model: Investigating the radiative impact of elevated point sources. *Atmos. Chem. Phys.* **2009**, *9*, 945–964. [CrossRef]
114. Chutia, L.; Ojha, N.; Girach, I.A.; Sahu, L.K.; Alvarado, L.M.A.; Burrows, J.P.; Pathak, B.; Bhuyan, P.K. Distribution of volatile organic compounds over Indian subcontinent during winter: WRF-chem simulation versus observations. *Environ. Pollut.* **2019**, *252*, 256–269. [CrossRef]
115. Willis, G.E.; Deardorff, J.W. A laboratory study of dispersion from a source in the middle of the convectively mixed layer. *Atmos. Environ.* **1981**, *15*, 109–117. [CrossRef]
116. Carruthers, D.J.; Edmunds, H.A.; Lester, A.E.; McHugh, C.A.; Singles, R.J. Use and validation of ADMS-Urban in contrasting urban and industrial locations. *Int. J. Environ. Pollut.* **2000**, *14*, 364–374. [CrossRef]
117. Li, M.; Yang, D.O.; Ho, W. Comparative study and prospect of Atmospheric diffusion model AERMOD and CALPUFF. *Geomat. Inf. Sci. Wuhan Univ.* **2020**, *45*, 1245–1254. [CrossRef]

118. Jokinen, T.; Sipila, M.; Richters, S.; Kerminen, V.M.; Paasonen, P.; Stratmann, F.; Worsnop, D.; Kulmala, M.; Ehn, M.; Herrmann, H.; et al. Rapid Autoxidation Forms Highly Oxidized RO2 Radicals in the Atmosphere. *Angew. Chem. Int. Ed.* **2014**, *53*, 14596–14600. [CrossRef]
119. Orlando, J.J.; Tyndall, G.S. Laboratory studies of organic peroxy radical chemistry: An overview with emphasis on recent issues of atmospheric significance. *Chem. Soc. Rev.* **2012**, *41*, 6294–6317. [CrossRef]
120. Hasson, A.S.; Tyndall, G.S.; Orlando, J.J.; Singh, S.; Hernandez, S.Q.; Campbell, S.; Ibarra, Y. Branching Ratios for the Reaction of Selected Carbonyl-Containing Peroxy Radicals with Hydroperoxy Radicals. *J. Phys. Chem. A* **2012**, *116*, 6264–6281. [CrossRef] [PubMed]
121. Atkinson, R. Atmospheric chemistry of VOCs and NOx. *Atmos. Environ.* **2000**, *34*, 2063–2101. [CrossRef]
122. Aumont, B.; Valorso, R.; Mouchel-Vallon, C.; Camredon, M.; Lee-Taylor, J.; Madronich, S. Modeling SOA formation from the oxidation of intermediate volatility n-alkanes. *Atmos. Chem. Phys.* **2012**, *12*, 7577–7589. [CrossRef]
123. Li, L.; Lu, C.; Chan, P.W.; Zhang, X.; Yang, H.L.; Lan, Z.J.; Zhang, W.H.; Liu, Y.W.; Pan, L.; Zhang, L. Tower observed vertical distribution of PM2.5, O_3 and NOx in the Pearl River Delta. *Atmos. Environ.* **2020**, *220*, 117083. [CrossRef]
124. Imhof, D.; Weingartner, E.; Vogt, U.; Dreiseidler, A.; Rosenbohm, E.; Scheer, V.; Vogt, R.; Nielsen, O.J.; Kurtenbach, R.; Corsmeier, U.; et al. Vertical distribution of aerosol particles and NOx close to a motorway. *Atmos. Environ.* **2005**, *39*, 5710–5721. [CrossRef]
125. Yang, X.Y.; Wang, X.H.; Yang, W.; Xu, J.; Ren, L.H.; He, Y.J.; Liu, B.; Bai, Z.P.; Meng, F.; Hu, M. Aircraft measurements of SO2, NOx, CO, and O3 over the coastal and offshore area of Yellow Sea of China. *Environ. Monit. Assess.* **2016**, *188*, 527. [CrossRef] [PubMed]
126. Han, S.Q.; Yao, Q.; Tie, X.X.; Zhang, Y.F.; Zhang, M.; Li, P.Y.; Cai, Z.Y. Analysis of surface and vertical measurements of O3 and its chemical production in the NCP region, China. *Atmos. Environ.* **2020**, *241*, 117759. [CrossRef]
127. Wang, Q.g.; Han, Z.; Wang, T.; Zhang, R. Impacts of biogenic emissions of VOC and NOx on tropospheric ozone during summertime in eastern China. *Sci. Total Environ.* **2008**, *395*, 41–49. [CrossRef] [PubMed]
128. Ho, K.F.; Lee, S.C.; Guo, H.; Tsai, W.Y. Seasonal and diurnal variations of volatile organic compounds (VOCs) in the atmosphere of Hong Kong. *Sci. Total Environ.* **2004**, *322*, 155–166. [CrossRef] [PubMed]
129. Dechapanya, W.; Russell, M.; Allen, D.T. Estimates of Anthropogenic Secondary Organic Aerosol Formation in Houston, Texas Special Issue of Aerosol Science and Technology on Findings from the Fine Particulate Matter Supersites Program. *Aerosol Sci. Technol.* **2004**, *38*, 156–166. [CrossRef]
130. Li, Q.Q.; Su, G.J.; Li, C.Q.; Liu, P.F.; Zhao, X.X.; Zhang, C.L.; Sun, X.; Mu, Y.J.; Wu, M.G.; Wang, Q.L.; et al. An investigation into the role of VOCs in SOA and ozone production in Beijing, China. *Sci. Total Environ.* **2020**, *720*, 137536. [CrossRef]
131. Jacobson, M.C.; Hansson, H.C.; Noone, K.J.; Charlson, R.J. Organic atmospheric aerosols: Review and state of the science. *Rev. Geophys.* **2000**, *38*, 267–294. [CrossRef]
132. Zhang, Z.J.; Wang, H.; Chen, D.; Li, Q.Q.; Thai, P.; Gong, D.C.; Li, Y.; Zhang, C.L.; Gu, Y.G.; Zhou, L.; et al. Emission characteristics of volatile organic compounds and their secondary organic aerosol formation potentials from a petroleum refinery in Pearl River Delta, China. *Sci. Total Environ.* **2017**, *584*, 1162–1174. [CrossRef]